framatome Non-Proprietary

COBRA-FLX: ORFEO-HMP Critical Heat Flux Correlation

ANP-10311NP-A,
Revision 1
Supplement 1NP
Revision 0

Topical Report

December 2021

Framatome Inc.

Non-Proprietary

Nature of Changes

Item	Section(s) or Page(s)	Description and Justification
1	All	Initial Issue

Contents

List of Tables

List of Figures

Nomenclature

Acronym	Definition
AFA-3G	AFA-3G grid design
ANOVA	Analysis of Variance
AOO	Anticipated Operational Occurrence
ARC	Alliance Research Center
BOHL	Beginning of Heated Length
BWR	Boiling Water Reactor
CE 14x14	Combustion Engineering type 14x14 fuel assembly design for PWRs
CE 16x16	Combustion Engineering type 16x16 fuel assembly design for PWRs
CEA	French Alternative Energies and Atomic Energy Commission
CHF	Critical Heat Flux
DL	Design Limit
DNB	Departure from Nucleate Boiling
DNBR	Departure from Nucleate Boiling Ratio
EOHL	End of Heated Length
GAIA	Framatome's PWR fuel assembly and grid design
GDC	General Design Criterion
HMP	HMP grid design
HTP	HTP grid design
HTRF	Columbia University's Heat Transfer Research Facility
IFM	Intermediate Flow Mixer
KATHY	Karlstein Thermal-Hydraulic test facility
LOOP	Loss of Offsite Power
M/P	Measured CHF divided by predicted CHF
MDNBR	Minimum Departure from Nucleate Boiling Ratio
MSLB	Main Steam Line Break
NMGRID	Non-mixing grid design
NRC	U.S. Nuclear Regulatory Commission
OD	Outer diameter
ORFEO	Framatome's CHF correlation form for PWR fuel assemblies
PWR	Pressurized Water Reactor
SER	Safety Evaluation Report
SRP	U.S. NRC Standard Review Plan
SSG	Simple Support Grid

TC	Thermocouple
W 15x15	Westinghouse type 15x15 fuel assembly design for PWRs
W 17x17	Westinghouse type 17x17 fuel assembly design for PWRs

Abstract

The HTP fuel assembly is equipped with structural grids (HTP) and may optionally include mid-span mixing grids called intermediate flow mixers (IFMs). The HTP and IFM grids have flow mixing devices (castellations). The lower end grid is an HMP grid, which does not have mixing devices.

This report documents a critical heat flux correlation as a supplement to the COBRA-FLX topical report. The CHF correlation is based on CHF tests performed for (i) several different grid designs without flow mixing devices, including HMP grids and (ii) HTP grids, including IFMs. This correlation is referred to as ORFEO-HMP. It is applicable to (i) fuel assemblies equipped with HMP and HTP grids, with or without IFMs and to (ii) the non-mixing grid region (HMP) on fuel assemblies equipped with mixing grids other than HTP. This report describes the correlation development, data sets, and the resulting application design limits and applicability ranges.

1.0 INTRODUCTION

The HTP fuel assembly is equipped with structural grids (HTP) and may optionally include mid-span mixing grids called intermediate flow mixers (IFMs). The HTP and IFM grids have mixing devices (castellations). The lower end grid is an HMP grid, which does not have mixing devices.

The HTP and HMP grids are used on Framatome fuel assemblies supplied to U.S. and European customers. The HTP grids provide lateral fuel rod support via a flow channel (castellation) located in the rod-to-rod gap (see Figure 1-1). At the outlet (downstream edge) of the grid, the flow through these channels is diverted from the vertical direction to promote increased thermal mixing in the subchannels. The IFM grid has flow mixing devices (castellations) similar to the HTP grid but has no structural functionality. The HMP grid features a linear fuel rod contact similar in concept to the HTP grid but has no mixing devices (the castellations are straight and the flow is not diverted from the vertical direction). The structure of the HTP fuel assembly including IFMs is illustrated in Figure 2-1.

This report describes the development and validation of a CHF correlation based on CHF tests performed for (i) several different grid designs without flow mixing devices, including HMP grids and (ii) HTP grids, including IFMs. This correlation is referred to as ORFEO-HMP.

The fuel designs in the CHF test data set include W 15x15, W 17x17, CE 14x14 and CE 16x16. The CHF test data consist of a wide range of pressures and mass fluxes, including low-pressure and low-flow statepoints. The correlation is applicable to nominal operating conditions and anticipated operational occurrences (AOOs) consistent with the applicability ranges for local conditions and fuel assembly geometry listed in Tables 2-2, 2-3, and 2-4.

The CHF correlation described in this report uses the ORFEO form, which is based on a modular approach that separates the general critical heat flux parameters from the fuel design specific

parameters. This is the same correlation form that was used in [1] for the ORFEO-GAIA and ORFEO-NMGRID correlations.

Section 2 of this report summarizes the statistical analysis and the applicability ranges for the ORFEO-HMP CHF correlation. Section 3 identifies the applicable regulatory requirements. Section 4 describes the CHF testing program. Section 5 discusses the code used for thermal-hydraulic simulations. Section 6 describes the generic ORFEO correlation and the specific grid parameters for the ORFEO-HMP correlation. Section 7 describes the statistical analysis performed based on the M/P CHF ratios, the calculation of the design limit (DL) and the determination of the application range for the correlation. Section 8 describes the quality assurance program applicable to the CHF testing and CHF correlation development and validation.

Framatome is requesting approval for the following:

- the ORFEO-HMP CHF correlation applied to fuel assemblies equipped with HMP and HTP grids, with or without IFMs as described in Section 2.2
- the ORFEO-HMP CHF correlation applied to the non-mixing grid region (HMP) on fuel assemblies equipped with mixing grids other than HTP.

Figure 1-1 HTP Mixing Grid Design Features

2.0 SUMMARY

2.1 ORFEO-HMP CHF correlation

Key statistical parameters of the ORFEO-HMP CHF correlation are provided in Table 2-1. The ORFEO-HMP CHF correlation is applicable to fuel assemblies equipped with non-mixing grids (HMP) and HTP grids, with or without IFM grids. The range of applicability is provided in Table 2-2 for ORFEO-HMP correlation with the Pressure-Velocity solver and Table 2-3 for ORFEO-HMP correlation with the SCHEME-Pressure solver (local thermal-hydraulic conditions) and Table 2-4 for both solvers (fuel assembly geometry). The ORFEO-HMP CHF correlation is applicable with the subchannel thermal-hydraulic analysis code COBRA-FLX.

Table 2-1 Key statistical parameters of the ORFEO-HMP correlation

Parameter	Value
Design limit	[ ]
Mean of the M/P population	[ ]
Standard deviation of the M/P population	[ ]

Table 2-2 Range of application for ORFEO-HMP correlation with the Pressure-Velocity solver (local thermal-hydraulic conditions)

Parameter	Units	Minimum value	Maximum value
Pressure	bar	19.5	179.6
	psia	282.8	2604.9
Mass flux	kg/m^{2}s	235.0	4650.0
	Mlbm/ft^{2}hr	0.1733	3.4286
Equilibrium quality	fraction	-0.6	0.8792

Table 2-3 Range of application for ORFEO-HMP correlation with the SCHEME-Pressure solver (local thermal-hydraulic conditions)

Parameter	Units	Minimum value	Maximum value
Pressure	bar	19.5	179.6
	psia	282.8	2604.9
Mass flux	kg/m^{2}s	248.7	4650.0
	Mlbm/ft^{2}hr	0.1834	3.4286
Equilibrium quality	fraction	-0.6	0.8769

Table 2-4 Range of application for ORFEO-HMP correlation (fuel assembly geometry)

2.2 Correlation application to the HTP fuel assembly

The ORFEO-HMP CHF correlation application to the HTP fuel assembly is illustrated in Figure 2-1. It is applicable to HTP fuel assemblies with or without IFMs. The ORFEO-HMP CHF correlation is also applicable to the non-mixing grid region (HMP) on fuel assemblies equipped with mixing grids other than HTP.

The non-mixing grid region is between the BOHL and the top plane of the first mixing grid. The mixing grid region is between the top plane of the first mixing grid and the EOHL.

Figure 2-1 Correlation application to HTP fuel assembly

3.0 REGULATORY REQUIREMENTS APPLICABLE TO THIS REPORT

Steady state and transient codes and methods used for licensing basis analyses are subject to regulatory requirements. The applicable regulation to this topical report is found in Title 10 of the U. S. Code of Federal Regulations (CFR), Part 50, Appendix A in General Design Criteria (GDC) 10. GDC 10 states, "the reactor core and associated coolant, control, and protection systems shall be designed with appropriate margin to assure that specified acceptable fuel design limits are not exceeded during any condition of normal operation, including the effects of anticipated operational occurrences".

Acceptable guidance for meeting the GDC 10 requirements is given in the U.S. NRC Standard Review Plan (SRP) (NUREG-0800) [2] in Section 4.4 for nuclear fuel "Thermal and Hydraulic Design." Section 4.4 of the SRP specifies the acceptance criteria to meet the relevant requirements of GDC 10. As it relates to this topical report for prediction of a Departure from Nucleate Boiling (DNB) condition, an example of how GDC 10 is met is stated below:

"For departure from nucleate boiling ratio (DNBR), CHFR or CPR correlations, there should be a 95-percent probability at the 95-percent confidence level that the hot rod in the core does not experience a DNB or boiling transition condition during normal operation or Anticipated Operational Occurrences (AOOs)."

The correlation and associated design limit in this report meet this criterion when used within the specified ranges of applicability.

4.0 CHF TESTING AND DATA

4.1 CHF test facilities

The phenomenon of CHF cannot be predicted from first principles; therefore, it is measured under laboratory conditions approximating those of an actual reactor core. A CHF correlation is developed based on these experimental measurements.

For PWR fuel assemblies, the CHF performance is measured by testing full length sections of the fuel assembly under reactor conditions. Electrically heated rods simulate the nuclear heating of fuel rods. The power of the test assembly is slowly increased until the boiling crisis is detected via a sudden increase in temperature. The critical power of the test assembly is measured as a function of system pressure, inlet mass flux and inlet temperature (subcooling). Depending on the local thermal-hydraulic conditions, both departure from nucleate boiling (DNB) and dryout phenomena can be observed.

The CHF tests (experiments) are conducted in test loops -- complex thermo-fluid systems capable of simulating the reactor core thermal-hydraulic conditions. The CHF testing programs for the CHF correlation developed and verified in this report use tests performed in four loops, as described below.

The tests performed at the Babcock and Wilcox's Alliance Research Center (ARC) test facility are identified with the prefix "AR". These tests supported the NRC-approved BWC and BWU-N CHF correlations in [3] and [4], respectively. The ARC tests AR6 - AR12 were part of the data set for the ORFEO-NMGRID correlation approved by the NRC in [1].

The tests performed at the Columbia University's Heat Transfer Research Facility (HTRF) are identified with the prefixes "CE", "EX", "SI" and "SP" with two exceptions: test SP010 was

performed in OMEGA and test SI700/1 was performed in KATHY. This facility has been extensively used as a source of CHF test data for correlations approved by the U.S. NRC (e.g., BWU-Z and BHTP approved in [4] and [5], respectively).

The CHF tests identified with the prefix "K" as well as test SI700/1 were performed in the KATHY loop -- Framatome's test facility located in Karlstein, Germany. Since 1986, KATHY has been extensively used to collect test data for licensing of PWR and BWR fuel assemblies. CHF tests performed in KATHY were used to license with the NRC the ACH-2 correlation, and the ORFEO-GAIA and ORFEO-NMGRID correlations in [6] and [1], respectively. A detailed description of the KATHY loop was provided in Section 4.1 of [1].

The test identified with the prefix "O" as well as test SP010 were performed in CEA's OMEGA loop located in Grenoble, France. The OMEGA test O1500 was part of the data set for the ORFEO-NMGRID correlation approved by the NRC in [1]. Information and a reference describing the OMEGA loop were provided in the response to RAI-SNPB-01 [1].

The qualification of KATHY as an acceptable source of CHF test data for CHF correlation development was provided with the ACH-2 CHF correlation in Section 2.2 of [6]. Additional benchmarking of the ARC, HTRF, KATHY and OMEGA test loops was provided in the response to RAI-SNPB-02 [1]. The benchmark validated the CHF test results obtained at each of these facilities for use in correlation licensing.

4.2 CHF test program

4.2.1 Test procedure and data collection methods

The test procedure and data collection methods for the new data supporting this report, obtained from the KATHY test loop, was provided in Section 4.2.1 of [1].

4.2.2 Test assembly configurations

All CHF tests, except for test SP510, were performed in a 5-by-5 rod configuration, which is the standard practice for PWR CHF testing (Table 4-3 and Table 4-4). Test SP510 was performed in a 6-by-6 rod configuration. Two configurations are tested: (i) unit subchannel and (ii) guide tube subchannel.

Each unit subchannel test assembly has 25 heater rods simulating the fuel rods (Figure 4-1, Figure 4-3, Figure 4-4, Figure 4-6, and Figure 4-11). Depending on the fuel assembly design, the guide tube subchannel test assembly can have the following configurations:

- 24 heater rods and 1 unheated rod located at the center of the matrix, simulating a small guide tube (Figure 4-2, Figure 4-12, and Figure 4-13).
- 22 heater rods and 3 unheated rods simulating small guide tubes (Figure 4-5)
- 21 heater rods and 1 unheated rod simulating a large guide tube (Figure 4-7, Figure 4-8, Figure 4-9, and Figure 4-10)
- 32 heater rods and 1 unheated rod located at the center of the matrix, simulating a large guide tube (Figure 4-14).

A unit subchannel is a channel adjacent to 4 heater rods. A guide tube subchannel is a channel adjacent to 3 heater rods and 1 guide tube. However, for the configurations with a large guide tube some guide tube subchannels are adjacent to 2 heater rods and 1 guide tube.

Table 4-3 and Table 4-4 list the geometry parameters for the non-mixing and mixing grid tests, respectively. The axial positions of the grids are shown in Appendix A. The non-uniform axial power profiles for the non-mixing and mixing grid tests are shown in Figure 4-15 and Figure 4-16,

respectively. The radial peaking factors for the non-mixing and mixing grid tests are shown in Table 4-1 and Table 4-2, respectively.

In an electrically heated test assembly with direct heater rods, electromagnetic forces are created. Therefore, it was necessary to strengthen the test assembly in order to ensure prototypic geometry was preserved under test conditions. For some test assemblies, the strengthening was achieved by (i) including simple support grids and (ii) placing motion limiters on the springs. The response to RAI-SNPB-08 [1] provides justification that the simple support grids do not artificially increase the CHF performance of the tested assemblies compared with the production assemblies.

Figure 4-1 Radial geometry of the 5-by-5 test section - unit subchannel configuration (tests AR6, AR8, AR11, K8500, K8800, O1500, AR16, O2400, K2200/1/2, K2300/1, K2600, K2900, K3100, K3800, K9100, K9300, and SP010)

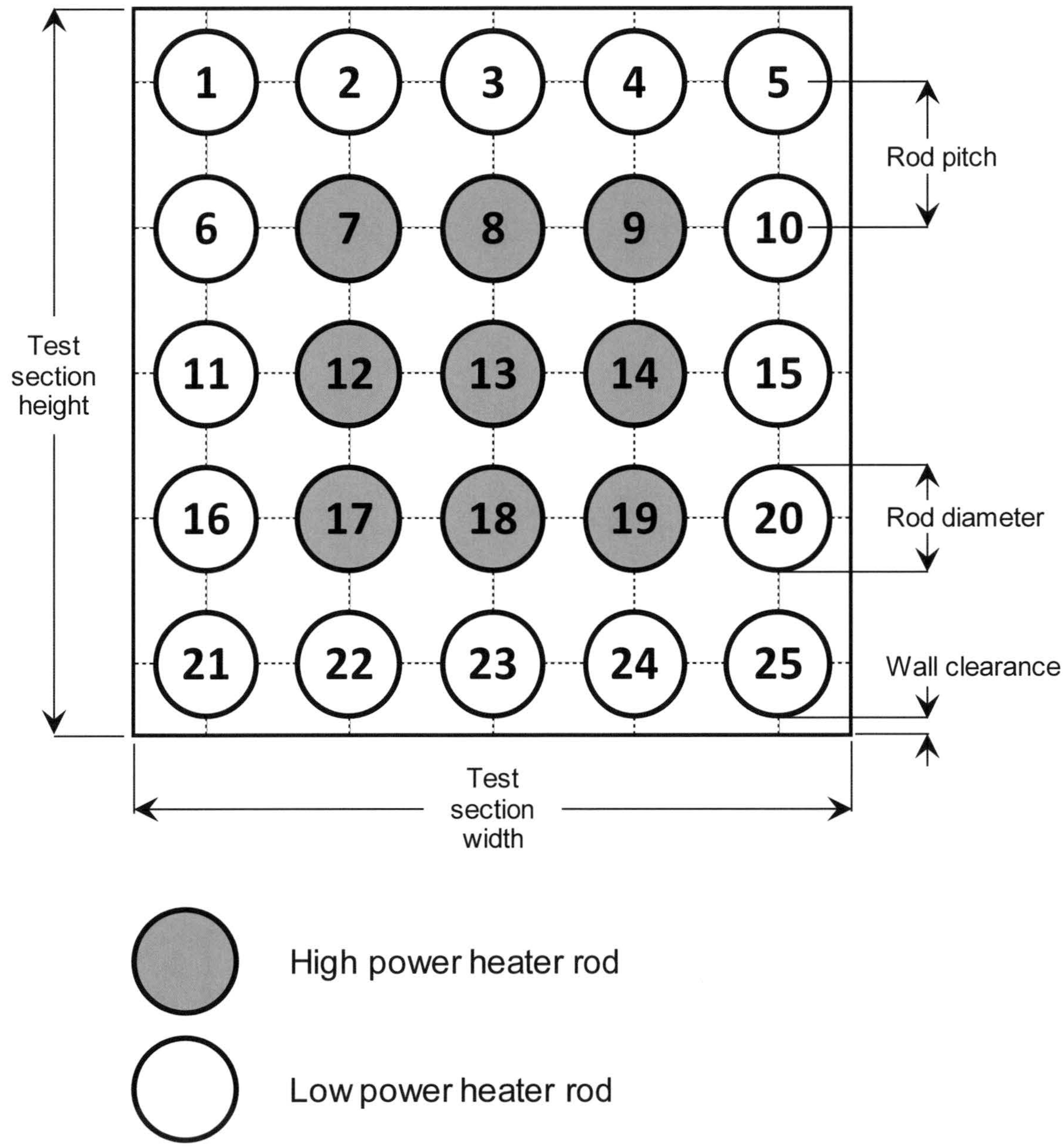

Figure 4-2 Radial geometry of the 5-by-5 test section - guide tube subchannel configuration (tests AR7, AR9, AR12, K6800, AR15, K2402, K2500, K3200, K4000/1, K9000, and K9200)

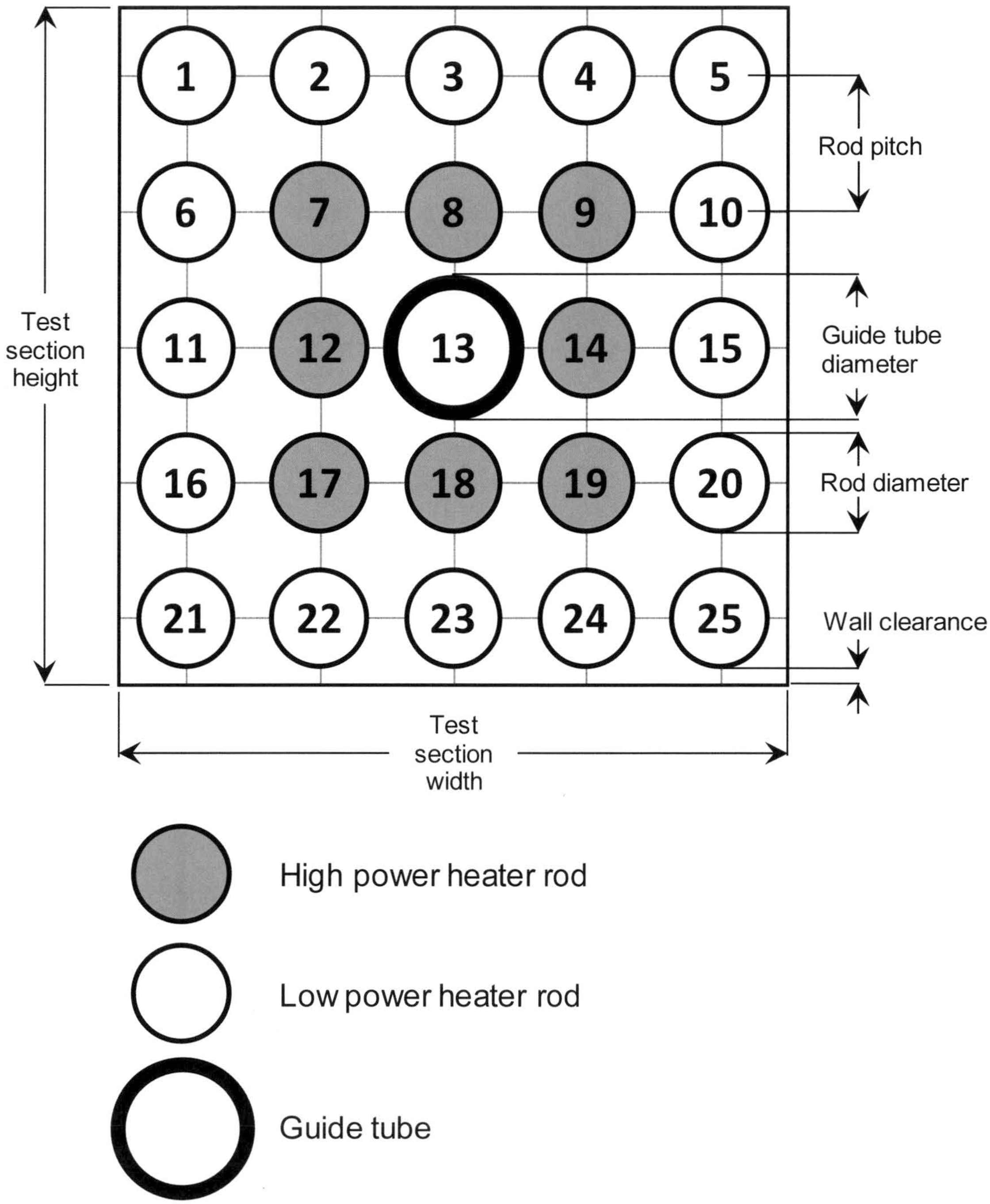

Figure 4-3 Radial geometry of the 5-by-5 test section - unit subchannel configuration (tests SI110/1, SI190, SI210, SI340, SI070, and SI320)

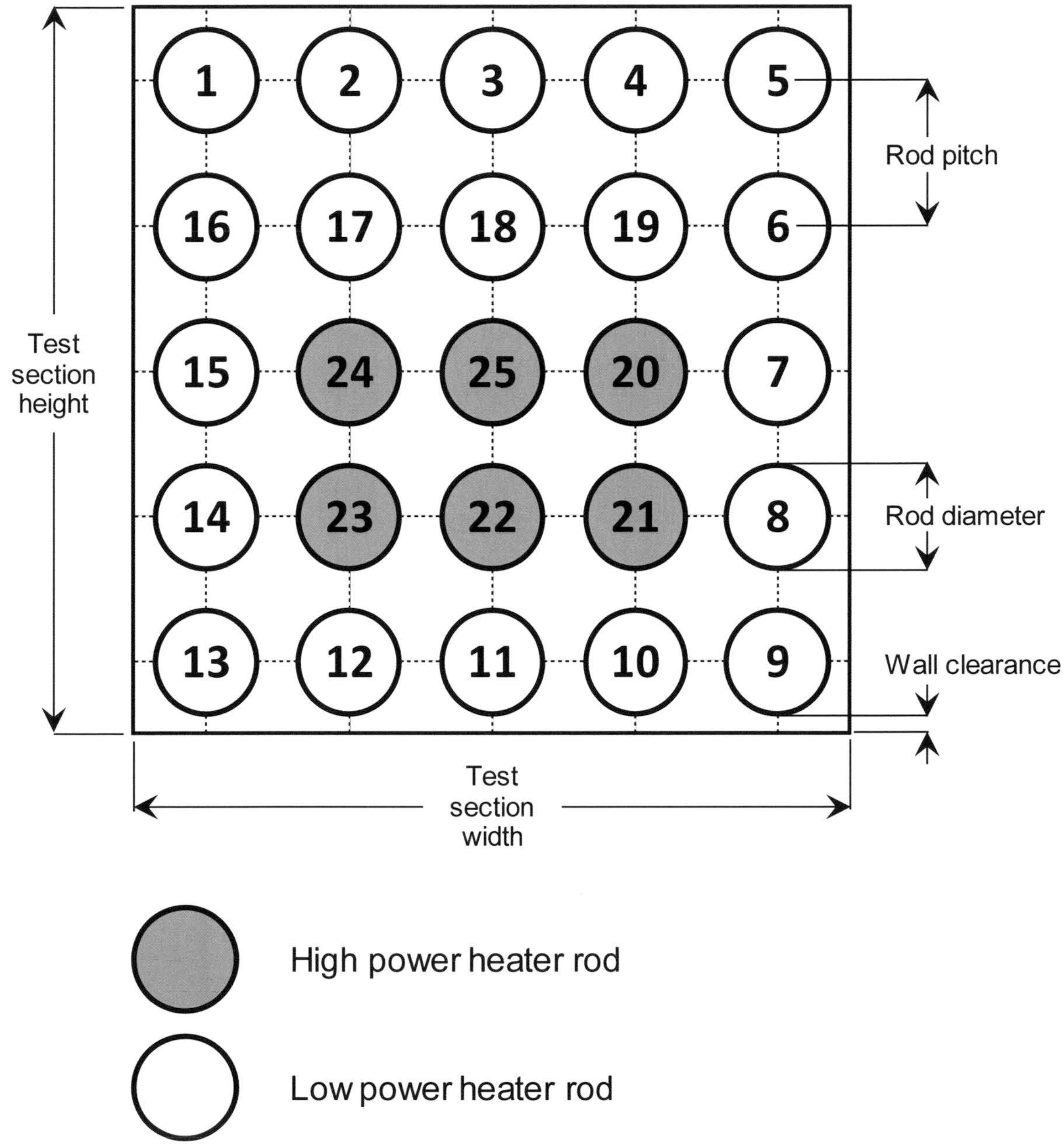

Figure 4-4 Radial geometry of the 5-by-5 test section - unit subchannel configuration (tests EX201, EX202, CE210, and CE480)

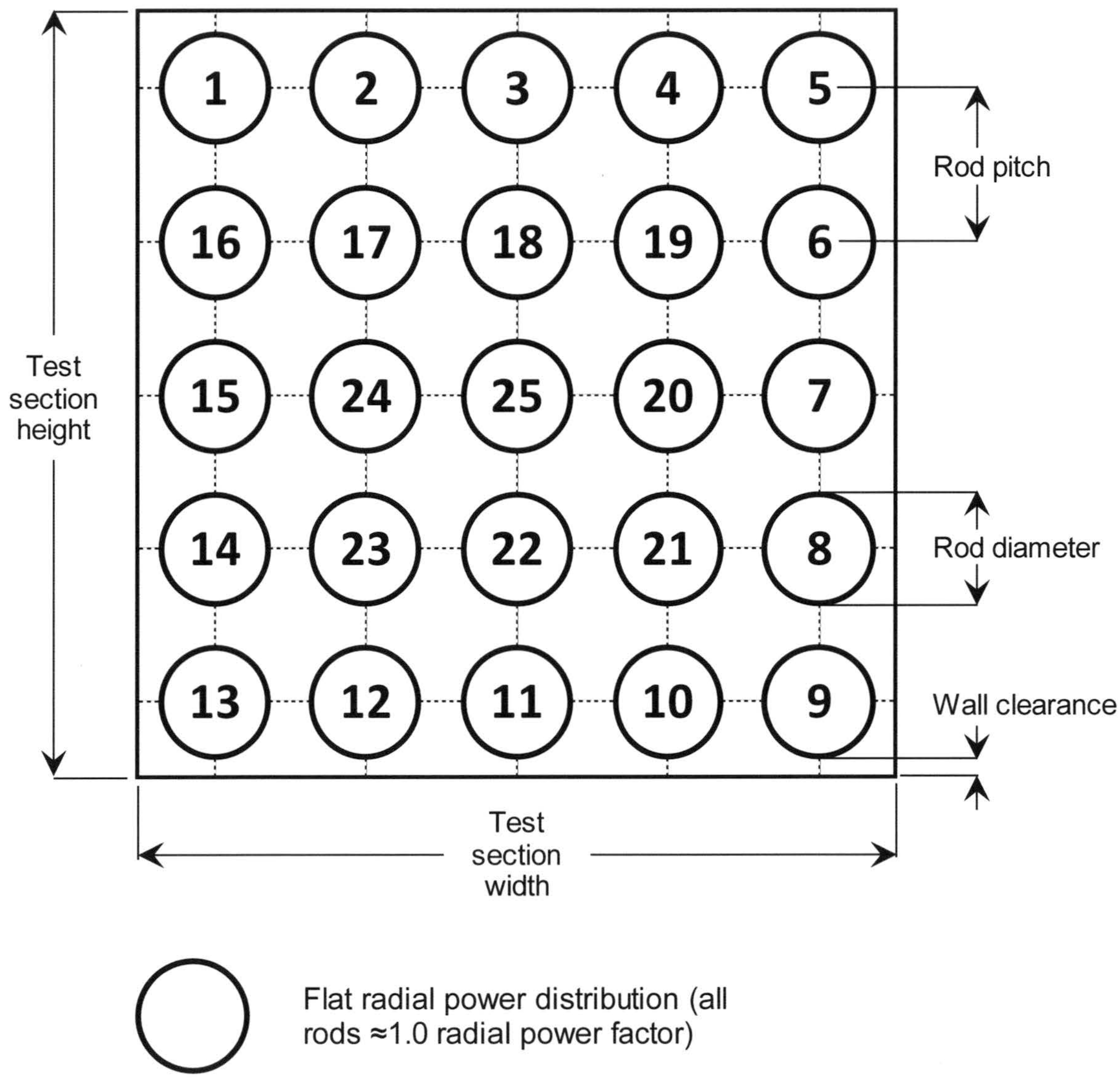

Figure 4-5 Radial geometry of the 5-by-5 test section - guide tube subchannel configuration (tests SI030, SI140, and SI160)

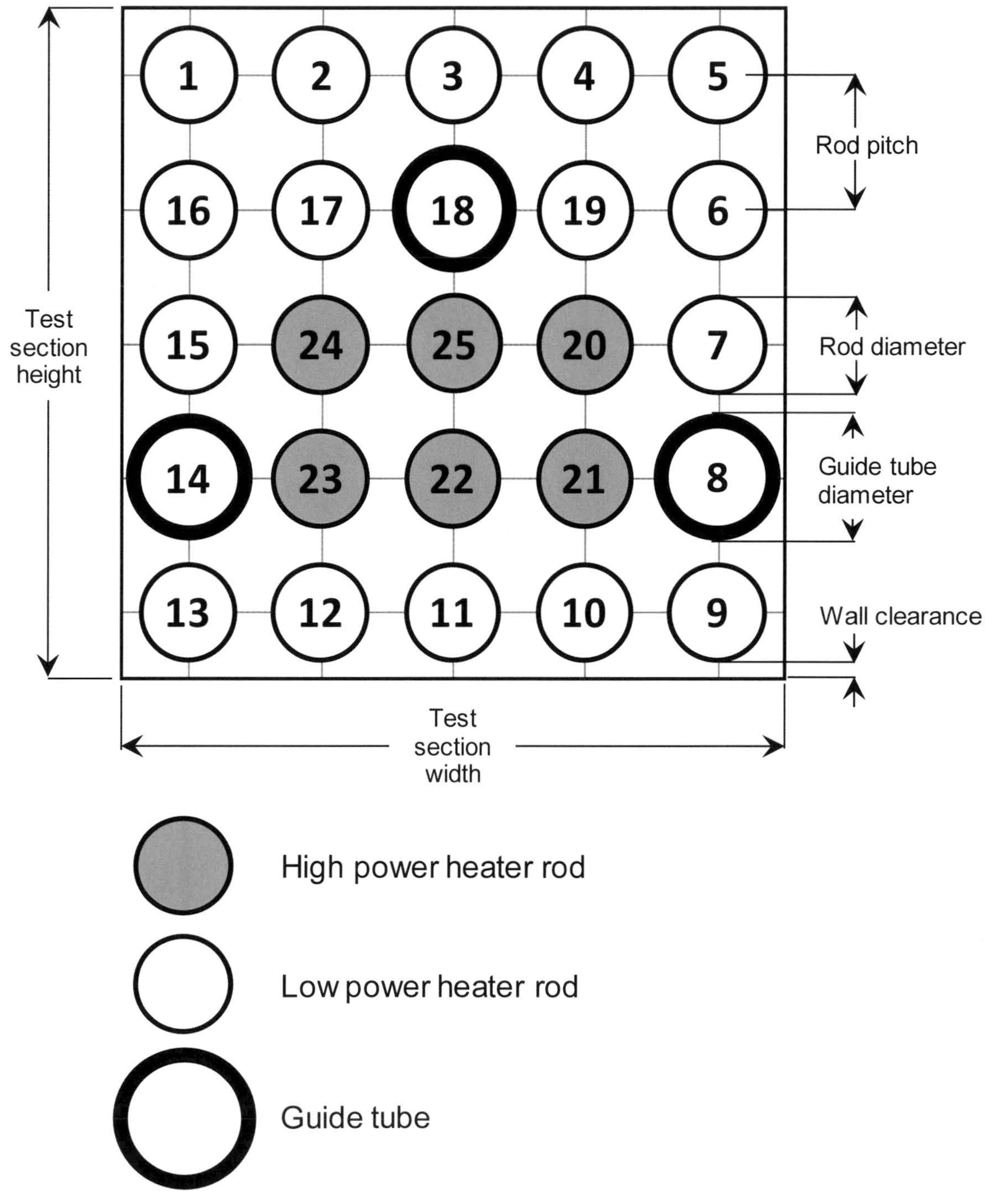

Figure 4-6 Radial geometry of the 5-by-5 test section - unit subchannel configuration (test CE130)

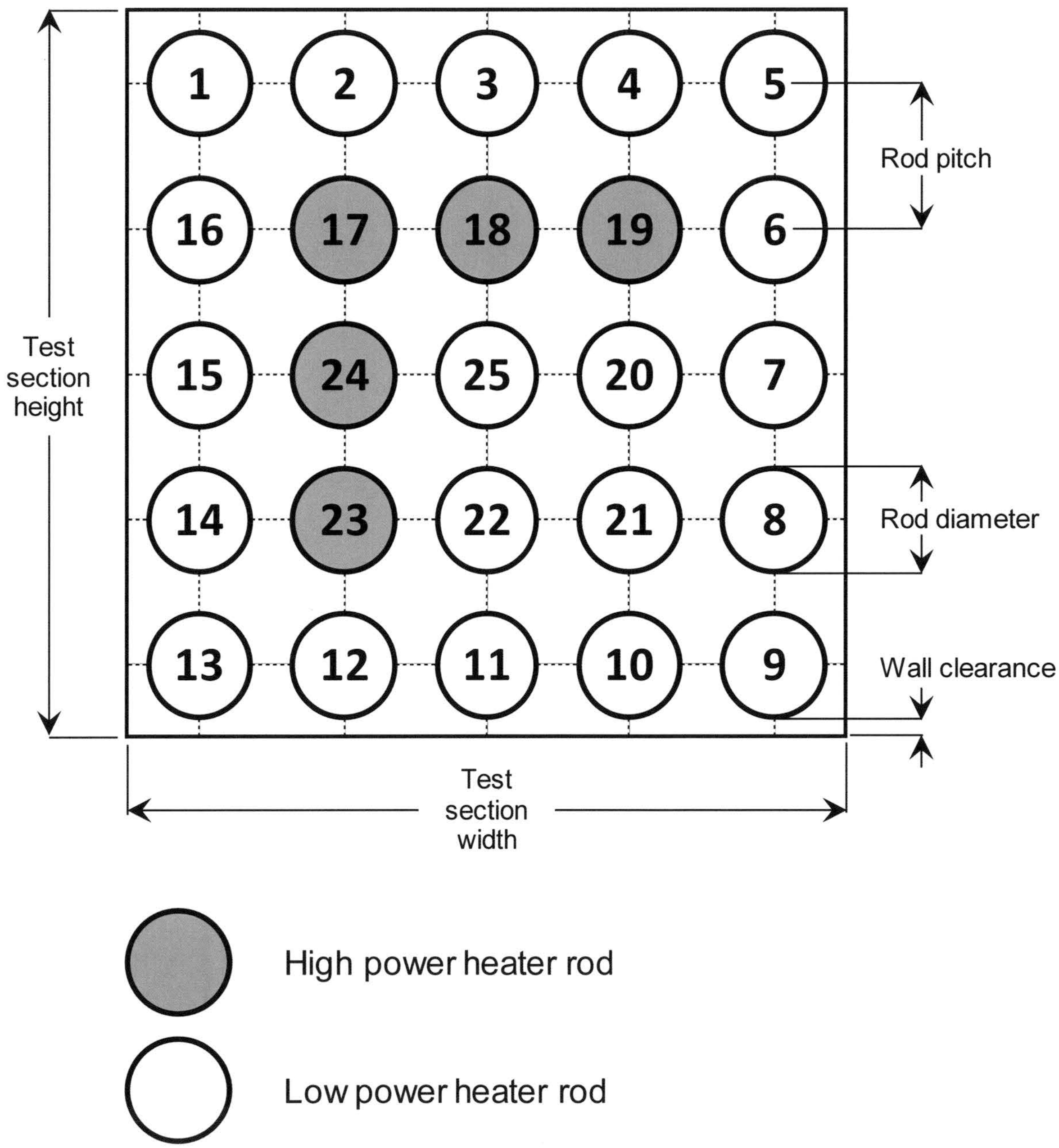

Figure 4-7 Radial geometry of the 5-by-5 test section - guide tube subchannel configuration (tests CE090, CE100, CE180, and CE190)

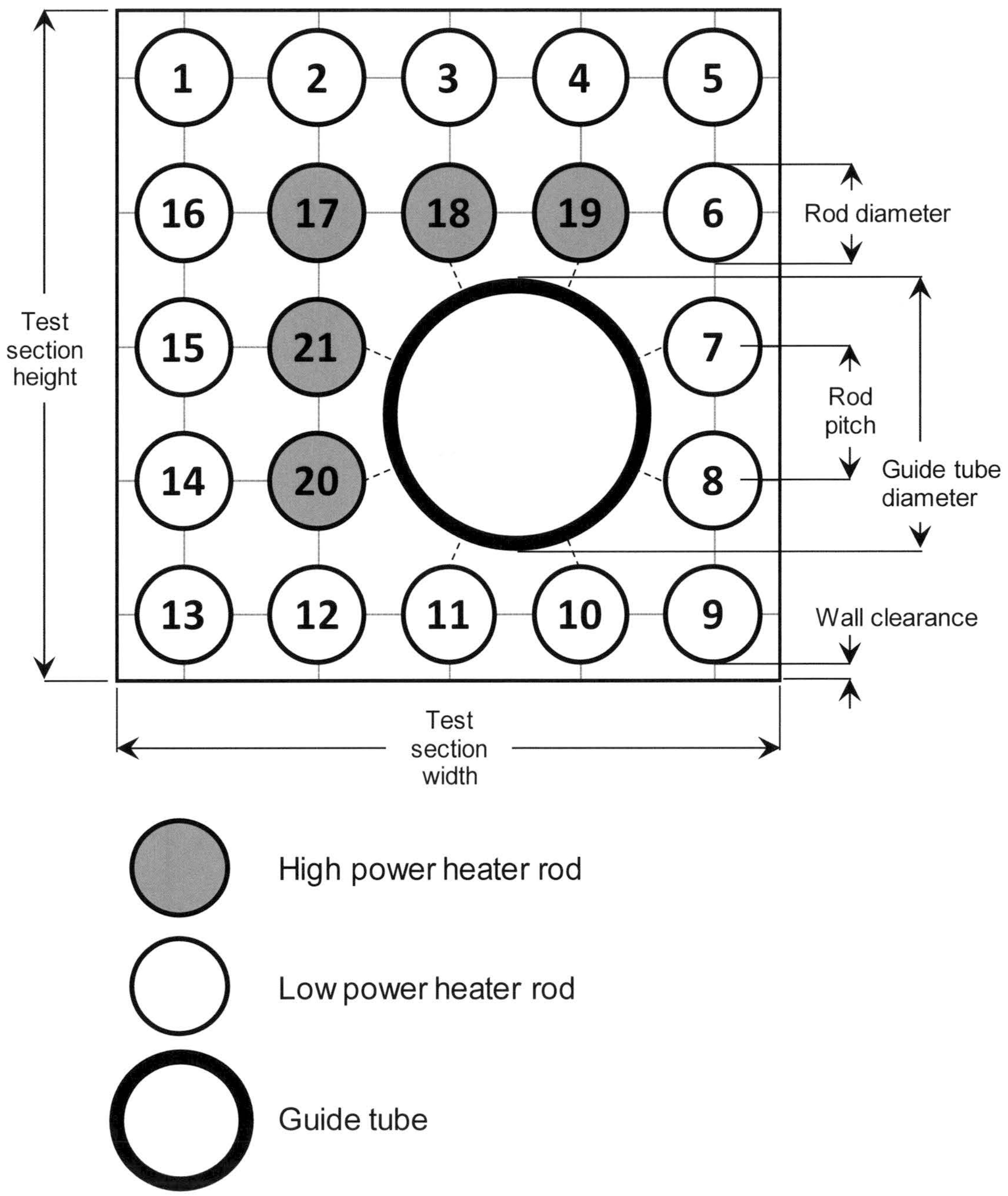

Figure 4-8 Radial geometry of the 5-by-5 test section - guide tube subchannel configuration (tests CE280, CE290, and CE580)

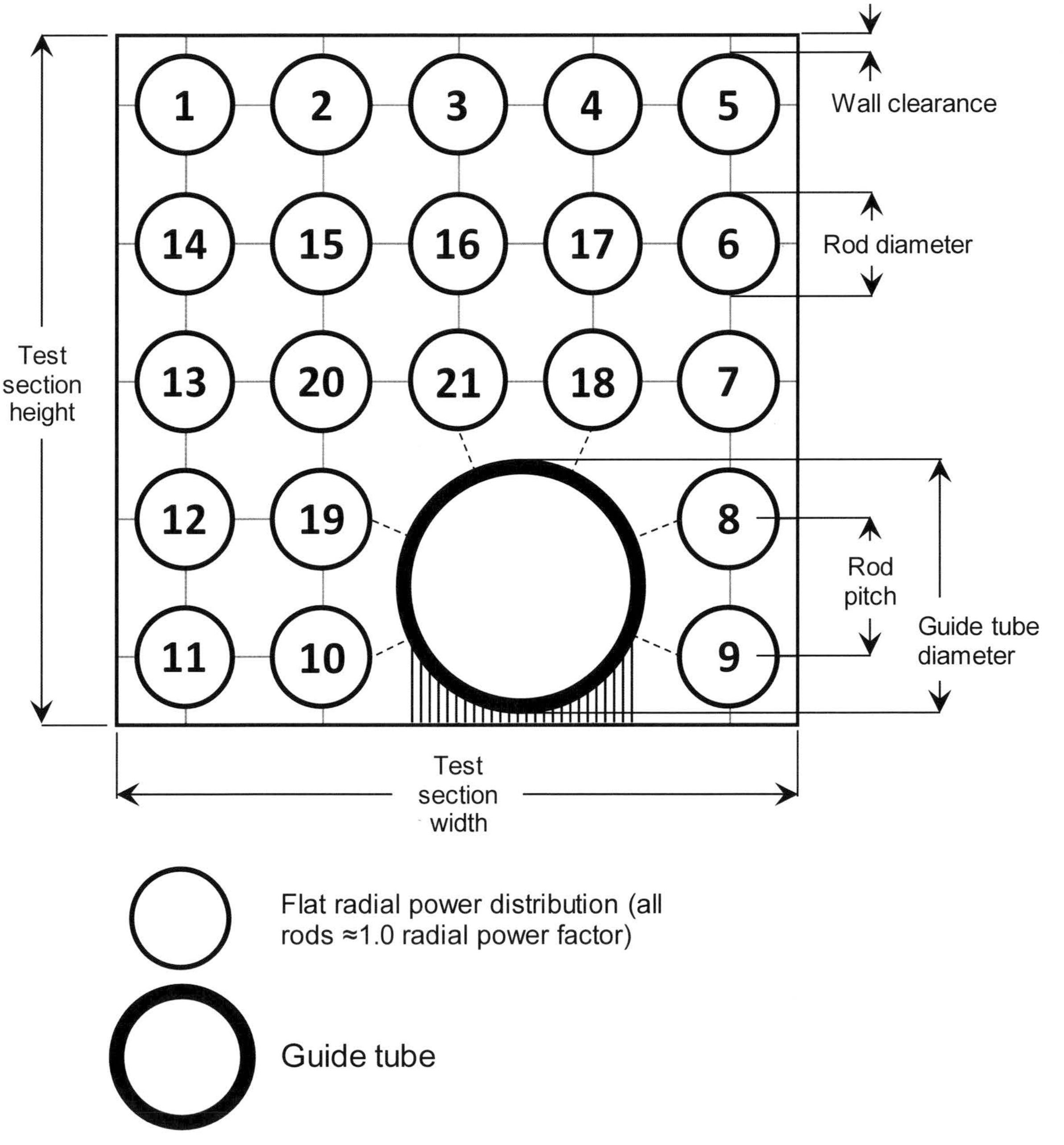

Figure 4-9 Radial geometry of the 5-by-5 test section - guide tube subchannel configuration (tests CE300, CE330, CE360/1, CE370, CE380,and CE600)

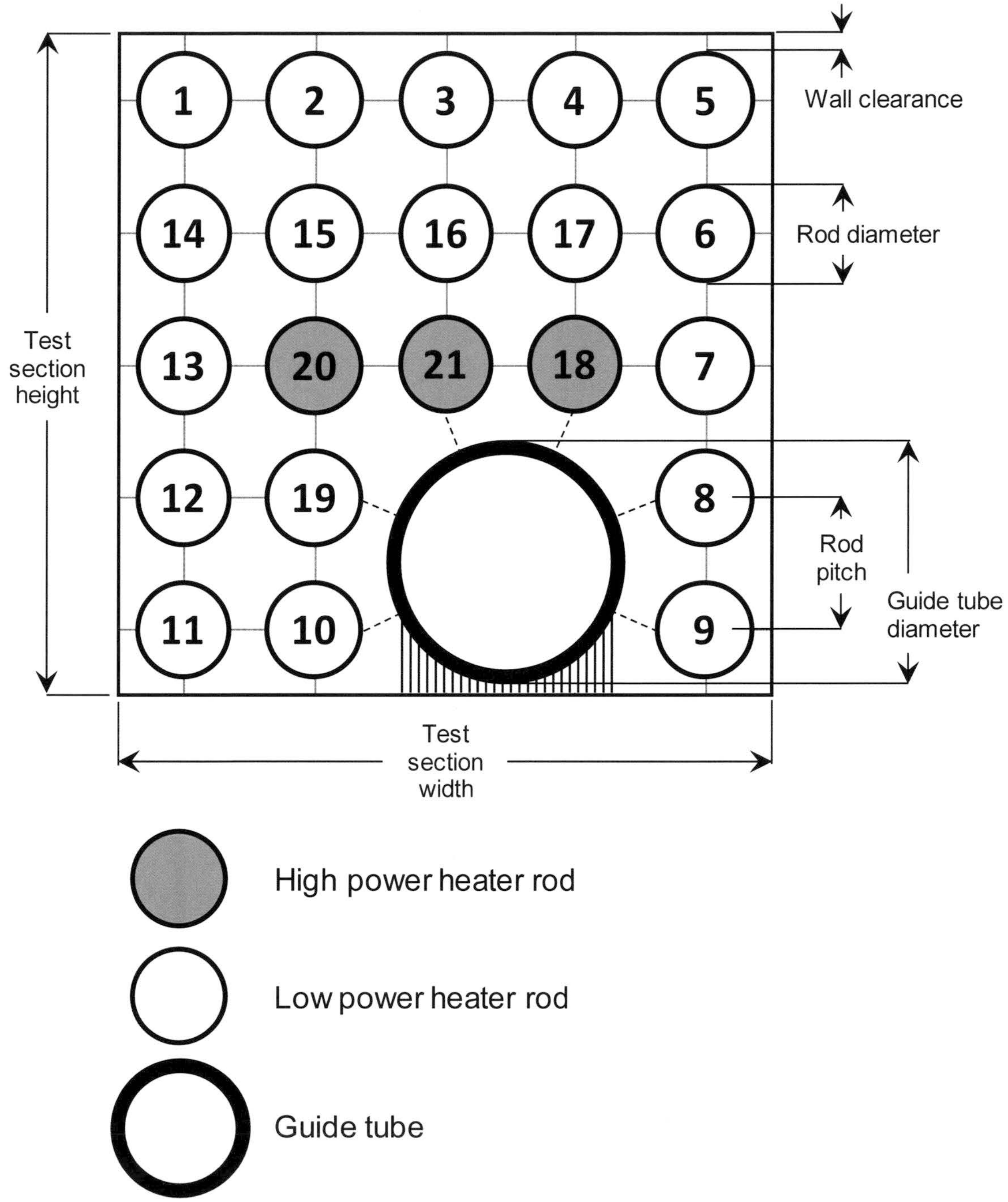

Figure 4-10 Radial geometry of the 5-by-5 test section - guide tube subchannel configuration (tests CE410, CE420, CE430, CE470, CE520/1, CE590, and CE660)

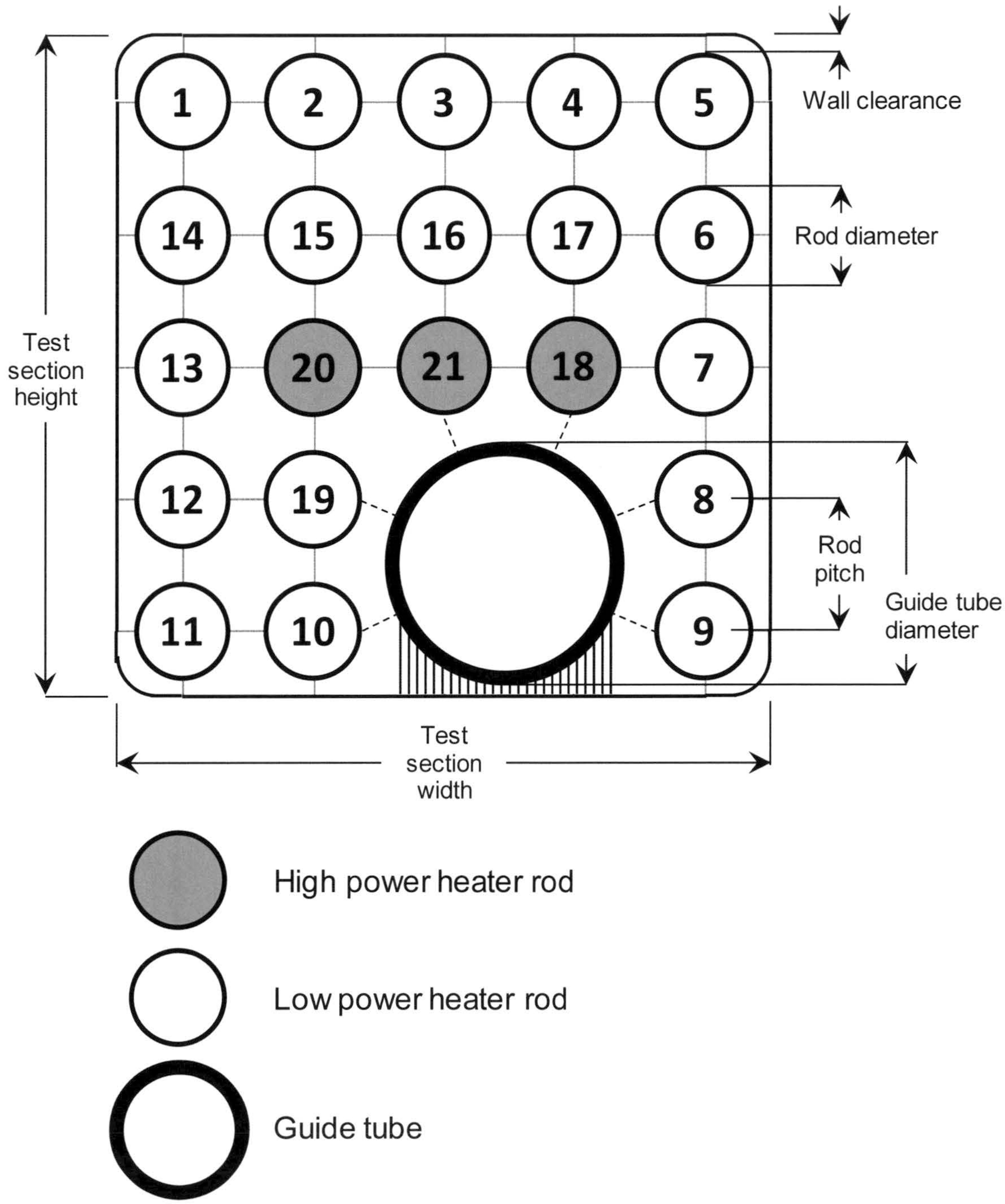

Figure 4-11 Radial geometry of the 5-by-5 test section - unit subchannel configuration (tests SP560, SP570, SP670, and SP690)

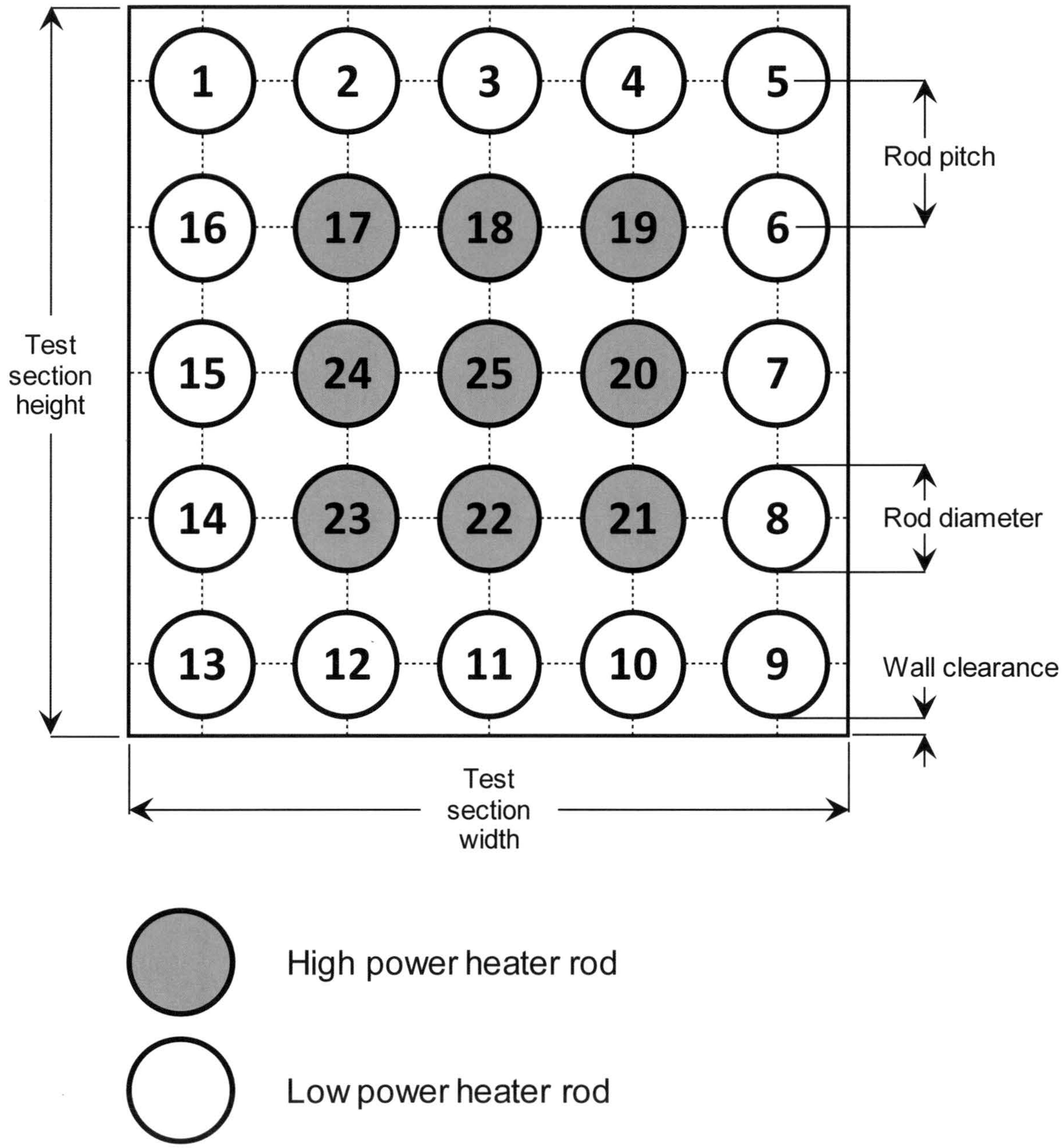

Figure 4-12 Radial geometry of the 5-by-5 test section - guide tube subchannel configuration (tests SP390, SP400 SP480, SP490, SP590/1/2, SP620, SP630, SP650/1, SP660 SP680, and SI700/1)

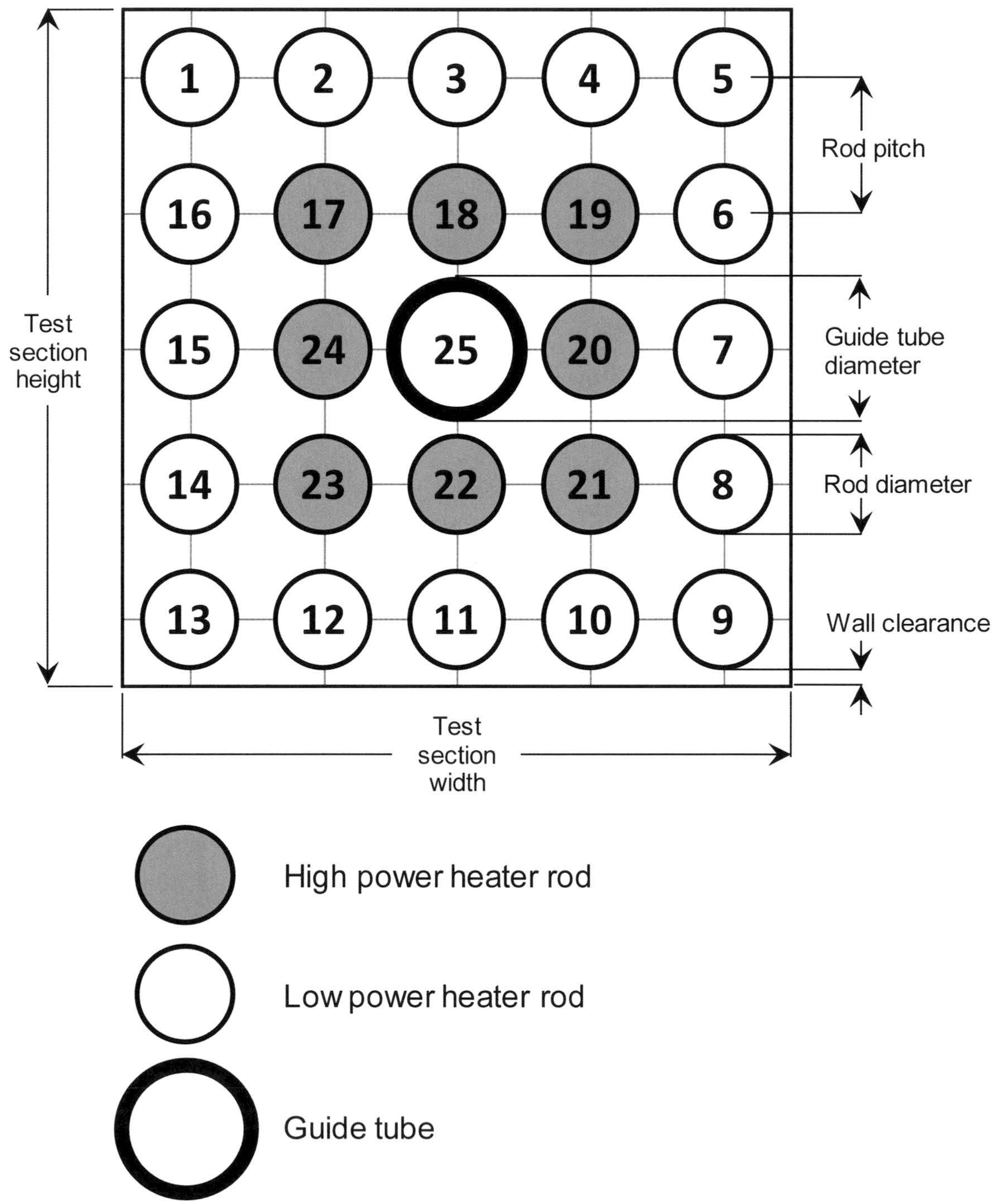

Figure 4-13 Radial geometry of the 5-by-5 test section - guide tube subchannel configuration (tests SP520 and SP530)

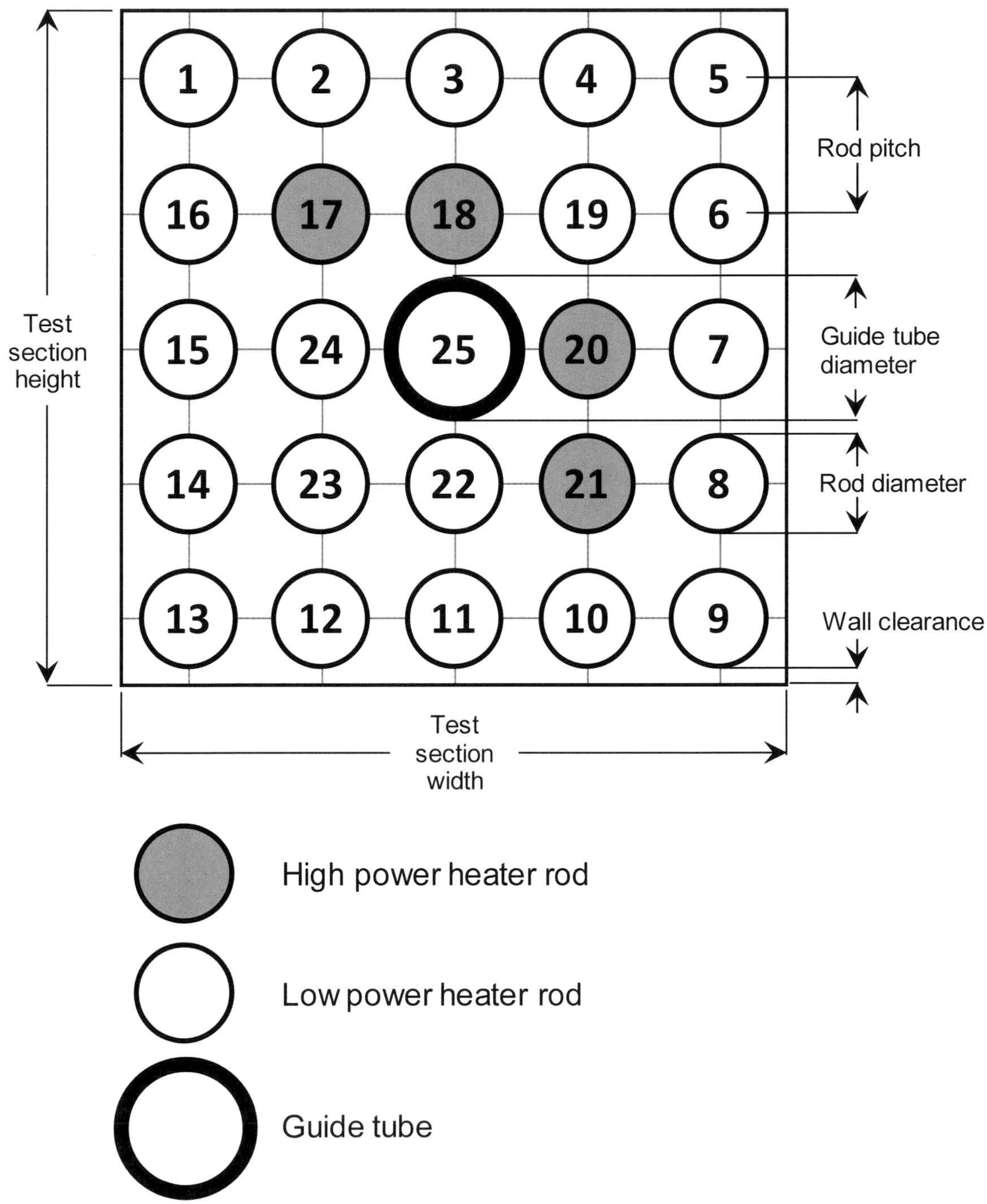

Figure 4-14 Radial geometry of the 6-by-6 test section - guide tube subchannel configuration (test SP510)

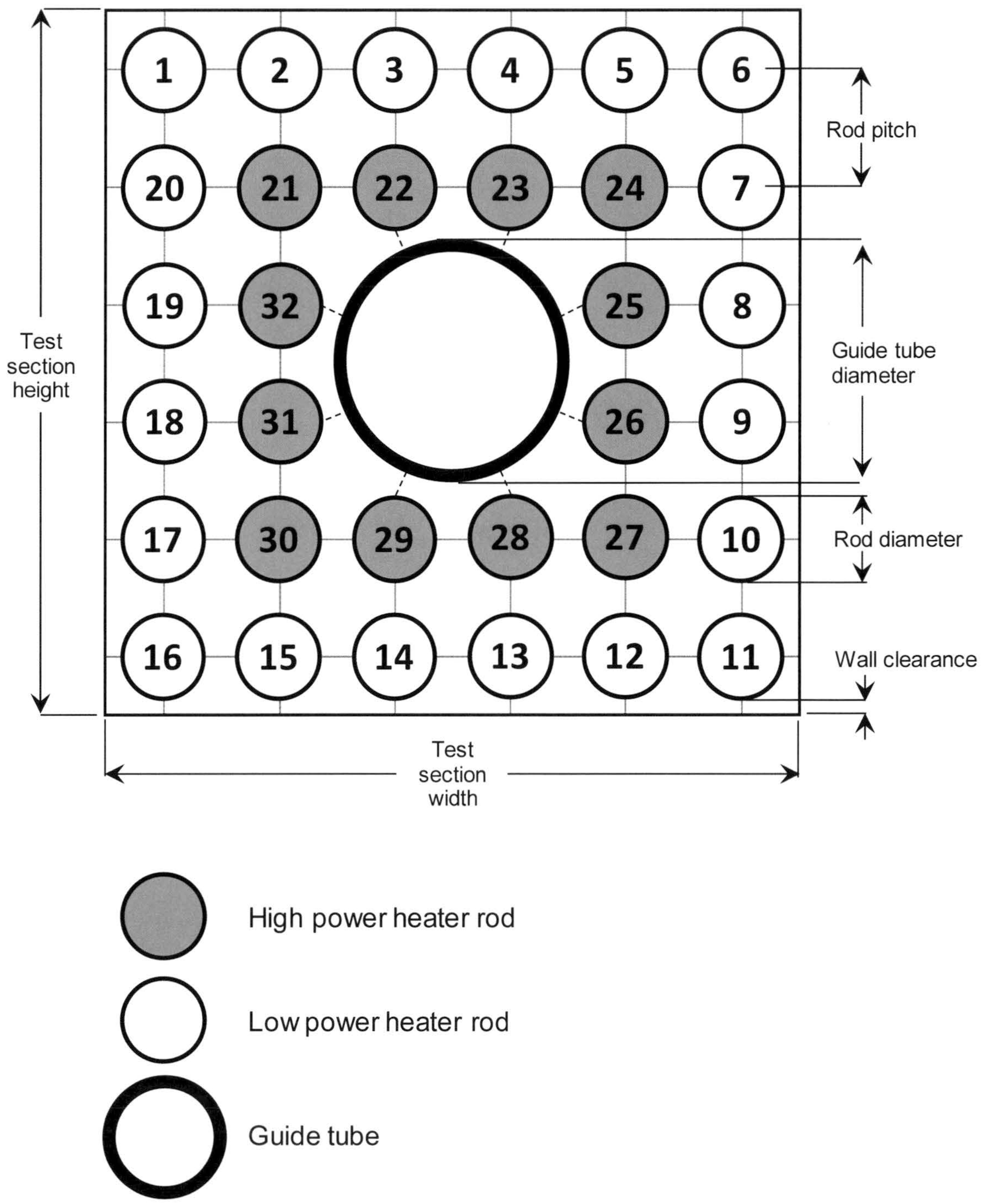

Figure 4-15 Axial power profiles for the non-uniform non-mixing CHF tests

Figure 4-16 Axial power profiles for the non-uniform HTP CHF tests

[

]

Table 4-1 Radial power factors for the non-mixing grid tests

[ ]

Table 4-1 Radial power factors for the non-mixing grid tests (continued)

Table 4-1 Radial power factors for the non-mixing grid tests (continued)

[ ]

Table 4-1 Radial power factors for the non-mixing grid tests (continued)

[ ]

Table 4-1 Radial power factors for the non-mixing grid tests (continued)

[ ]

Table 4-1 Radial power factors for the non-mixing grid tests (continued)

[ ]

Table 4-2 Radial power factors for the HTP tests

[ ]

Table 4-2 Radial power factors for the HTP tests (continued)

Table 4-2 Radial power factors for the HTP tests (continued)

Table 4-2 Radial power factors for the HTP tests (continued)

[ ]

Table 4-2 Radial power factors for the HTP tests (continued)

[ ]

4.2.3 CHF test program design -- non-mixing grid

The non-mixing CHF test matrix supporting the ORFEO-HMP CHF correlation is shown in Table 4-3. Tests K8500 and K8800 feature [ ] The data set covers [ ] Their common feature is [ ] The majority of these CHF tests were previously used in other NRC-approved CHF correlations as following:

- tests with the prefix "AR": BWC [3], BWU-N [4]
- tests AR6 - AR12, K6800, K8500, O1500, SI110/1, SI190, SI210, SI340: ORFEO-NMGRID [1]
- tests with the prefix "CE": ABB-NV and/or WLOP [7] and [8]

Table 4-3 Geometry of the non-mixing grid tests

Table 4-3 Geometry of the non-mixing grid tests (continued)

4.2.4 CHF test program design -- mixing grid (HTP grid)

The HTP CHF test matrix supporting the ORFEO-HMP CHF correlation is shown in Table 4-4. All tests feature HTP grids and some tests include IFMs. The data set covers [ ]. The majority of these CHF tests were previously used in other NRC-approved CHF correlations as following:

- tests K2200 - K4001, except K2202: ACH-2 [6]
- tests K9000 - K9300: NuScale [9]
- tests with prefix "SP" except SP010 and SP660: BHTP [5]

Table 4-4 Geometry of the HTP tests

Table 4-4 Geometry of the HTP tests (continued)

[ ]

4.2.5 Data collection ranges

The development of a CHF correlation requires the acquisition of a data set that covers the application domain with a sufficient data density with an acceptable uncertainty. Pressure, mass flux and inlet temperature (subcooling) were all considered in developing the testing strategy to ensure that the application domain is adequately covered. An expanded coverage of the application domain in quality was achieved by collecting CHF statepoints characterized by a combination of high pressure and low inlet subcooling. This leads to local conditions characterized by high equilibrium quality (Figure 7-25). CHF statepoints characterized by low pressure and low flow were included in order to ensure the correlation applicability in this range.

4.3 CHF test data

Table B-1 contains the assembly conditions for the non-mixing CHF statepoints that are part of the data set of the ORFEO-HMP correlation.

Table B-2 contains the assembly conditions for the HTP CHF statepoints that are part of the data set of the ORFEO-HMP correlation.

Table B-3 contains the calculated local conditions for the CHF statepoints (non-mixing grid and HTP grid) that are part of the data set of the ORFEO-HMP correlation.

5.0 SUBCHANNEL CODE

The PWR CHF correlations are developed based on local thermal-hydraulic conditions. The local thermal-hydraulic conditions are calculated by a subchannel code. The ORFEO-HMP correlation is developed and verified using the subchannel code COBRA-FLX, which has been reviewed and approved by the U.S. NRC for application to nuclear core thermal-hydraulic analysis for steady-state and transient conditions in [10]. The subchannel code modeling requirements used for developing the ORFEO-HMP correlation with COBRA-FLX are established based on the empirical correlations and numerical solution methods approved by the U.S. NRC in the SER issued for the COBRA-FLX Topical Report [10] and listed in Table 5-1.

Table 5-1 Empirical correlations and numerical solution methods used in the COBRA-FLX subchannel code model

Parameter	Value
Conservation equations solver	Pressure-Velocity or SCHEME-Pressure
Water properties	IAPWS-IF97
Subcooled void correlation	Saha-Zuber
Bulk void correlation	Chexal-Lellouche using the full curve fit routine or interpolation table
Two-phase friction multiplier	Homogeneous model
Wall friction factor	Standard model
Wall friction correction	Wall viscosity correction included in the wall friction factor
Subcooled boiling profile fit	Zuber-Staub
Turbulent mixing coefficient [1]	[ ] for the non-mixing grids [ ] for the HTP grids
Diversion crossflow resistance factor	0.15
Turbulent momentum factor	1.0
Transverse momentum parameter	0.25

Note: 1. The mixing behavior of the spacer grids is modeled via diffusion of energy (turbulent enthalpy exchange without mass exchange) across the gaps between subchannels. The turbulent mixing coefficients are determined from mixing tests performed with the CHF test assemblies. Thermocouples are attached at the exit of the test assembly and subchannel temperature distribution is measured in single phase flow. The mixing coefficient is the value that minimizes the difference between measured temperatures and COBRA-FLX predicted temperatures.

6.0 CORRELATION DEVELOPMENT

6.1 Background

In PWR cores, energy is generated by uranium dioxide fuel pellets enclosed in fuel rods. The energy leaves the fuel rod surface in the form of heat flux, which is removed by the coolant system flow. The normal mode of heat transfer to the coolant at high power densities is nucleate boiling. Nucleate boiling is an efficient mode of heat transfer, with heat transfer coefficients about 280,000 W/m^2K.

As the capacity of the coolant to accept heat from the fuel rod surface and transfer it by bubble detachment to the coolant stream degrades, a continuous layer or film of steam starts to blanket the rod. The steam film insulates the rod and the heat transfer coefficient drops drastically to around 2800 W/m^2K. This is because the heat transfer mechanism is film boiling, primarily conduction through the steam layer.

Reactor cores must be protected against possible damage that could result from the high clad temperatures that are experienced in the transition to, and during, film boiling. The heat flux at which the steam film starts to form is termed the critical heat flux or the point of departure from nucleate boiling (DNB).

For design purposes, the departure from nucleate boiling ratio (DNBR) is used as an indicator of the margin to DNB. The DNBR is the ratio of the predicted CHF to the actual heat flux at the same condition. Therefore, the DNBR is a measure of the thermal margin to film boiling and its associated high temperatures. In general, a higher DNBR value leads to a higher thermal margin.

The CHF cannot be predicted from first principles, so it is empirically correlated as a function of the local thermal-hydraulic conditions, the geometry and the power distribution measured in

experiments. CHF test data are typically obtained from experiments under steady state conditions. It is common practice, based on experimental evidence, to assume the CHF, during a transient situation, will be exceeded when the local instantaneous conditions are equivalent to those causing its occurrence under steady-state conditions, as discussed in Section 9.6.2 of [11]. Because a CHF correlation is essentially a surface fit to experimental data, it has an associated uncertainty. This uncertainty is quantified in a DNBR design limit, consistent with the specified acceptable fuel design limit discussed in [2]. A calculated DNBR value greater than this design limit ensures that there is, at a minimum, a 95% probability with 95% confidence (95/95) that a departure from nucleate boiling will not occur. [

]

Framatome has developed and continues to use numerous CHF correlations for its fuel assemblies. The two most recently reviewed and approved by the U.S. NRC are the ORFEO-GAIA and ORFEO-NMGRID correlations [1]. The CHF correlation described in this report is based on the same correlation form used for ORFEO-GAIA and ORFEO-NMGRID, called ORFEO. The ORFEO correlation form introduced improvements to reduce variability of the measured-to-predicted CHF ratio.

6.2 ORFEO CHF correlation form

The ORFEO CHF correlation utilizes a modular approach that separates the general representation parameters from the grid specific parameters. This approach is similar to the generalized subchannel CHF correlation for PWR and BWR fuel assemblies presented in [12] and the

introduction of correction factors to extend the Groeneveld CHF tables in [13] to rod bundle geometries [14].

A detailed description of the ORFEO correlation form is provided in Section 6.2 of [1].

The functional form of the ORFEO CHF correlation is the following:

$$CHF = \frac{F_{BASE}(P, G, X, Z_{BO}) \cdot F_{SPACER}(P, G, X, \text{Geometry})}{FNU}$$

where:

F_{BASE}	- CHF general representation term, based on local conditions, MW/m^2
F_{SPACER}	- fuel design specific multiplier, based on grid specific design
FNU	- axial power factor, accounts for non-uniform axial power profiles

The F_{BASE} term incorporates the generic dependency on local thermal-hydraulic conditions (pressure, mass flux, effective quality) and burnout length (Z_{BO}). The F_{BASE} term developed for ORFEO-GAIA and ORFEO-NMGRID in Section 6.2 of [1] is used for ORFEO-HMP and it is repeated here for convenience.

[ ]

where:

[ ]

The normalized pressure and mass flux are defined:

[ ]

where:

P - system pressure (bar)

G - local mass flux $\frac{kg}{m^2 \cdot s}$

The values of the "a" and "b" coefficients are listed in Table 6-1.

The quality functions are defined as follows:

[ ]

where X is the effective quality.

The effective quality incorporates the burnout length term and is defined:

[ ]

where:

X_{eq} - local equilibrium quality (fraction)

Z_{BO} - burnout length (m)

Table 6-1 Coefficients in F_{BASE} term

[ ]

The ORFEO correlation form incorporates an axial power factor, FNU to describe the memory effects observed when comparing CHF test data based on uniform versus non-uniform axial power profiles. The axial power factor is based on Tong's formulation [15]. The axial power factor term developed for ORFEO-GAIA and ORFEO-NMGRID in Section 6.2 of [1] is used for ORFEO-HMP and it is repeated here for convenience.

$$FNU(l_{DNB}) = \frac{K}{\varphi(l_{DNB}) \cdot (1 - e^{-K \cdot l_{DNB}})} \cdot \int_0^{l_{DNB}} \varphi(Z) \cdot e^{-K \cdot (l_{DNB} - Z)} dZ$$

$$K = \frac{b_1 \cdot (1 - X_{eq})^{b_2}}{\left(\frac{G}{1000}\right)^{b_3}}$$

where:

l_{DNB} - elevation where CHF is calculated (m)

Z - elevation (m)

$\varphi(Z)$ - local heat flux $\left(\frac{MW}{m^2}\right)$

In the above equation, the integration interval starts at the beginning of the heated length. [ ] The coefficients of the empirical factor K are fitted to reflect the overall description of non-uniform axial power profiles in the ORFEO correlation form via [ ] The values of the "b" coefficients in the FNU term are listed in Table 6-2.

Table 6-2 Coefficients in FNU term

[ ]

[ ] It can be viewed as an initial approximation of the CHF performance of a particular grid design. The F_{SPACER} term can be viewed as an adjustment applied to the generic part of the ORFEO correlation in order to reflect the CHF performance of a particular grid design. The fitting process of the F_{SPACER} term is based on CHF test data collected for that particular grid design.

The F_{SPACER} term incorporates the specific CHF dependency of the fuel assembly geometry and spacer grid design. The form of the F_{SPACER} term is the following:

[ ]

The distance-to-grid effect is modeled using [

] as follows:

[

]

where:

dg –distance-to-grid (distance from the elevation where CHF is calculated to the elevation of the bottom edge of the upstream grid; see Figure 6-1) (m).

$l_{grid,1}$ – decay length coefficient defined in Table 6-5 (m).

All structural and intermediate grids (with or without mixing features) are included when deriving the F_{GRID} term.

The guide tube impact accounts for the difference in measured CHF performance between the guide tube subchannel and the unit subchannel of a grid:

[

]

where rtg is [

]

The effect of grid spacing is modeled using [ ] The grid spacing term is calculated as follows:

[ ]

where:

gsp —grid spacing (lower edge-to-lower edge distance between two consecutive grids); see Figure 6-1 (m)

$l_{grid,2}$ – decay length coefficient defined in Table 6-5 (m).

The grid spacing is based on the [ ] this includes the case when CHF is calculated in the span that contains the end of heated length. When CHF is calculated [ ]

Section 6.3 describes the development process for the ORFEO-HMP correlation.

Figure 6-1 Definition of grid spacing and distance-to-grid

6.3 ORFEO-HMP CHF correlation

The non-mixing grid CHF test data set is described in Table B-1. In order to develop and validate the ORFEO-HMP correlation, the non-mixing grid part of the CHF test data set is divided as follows:

Table 6-3 provides the number of statepoints from each test in each partition. The partitions were generated using a random selection process.

Table 6-3 Number of statepoints in the defining and validation data sets of the non-mixing grid CHF test

Table 6-3 Number of statepoints in the defining and validation data sets of the non-mixing grid CHF test (continued)

The HTP CHF test data is described in Table B-2. This is used exclusively for validation of the correlation with no contribution to the defining data set (see Table 6-4).

Table 6-4 Number of statepoints in the validation of the HTP grid CHF test data sets

Table 6-4 Number of statepoints in the validation of the HTP grid CHF test data sets (continued)

[ ]

Figure 6-2, Figure 6-3 and Figure 6-4 show the distribution of defining and validation data sets in terms of pressure, mass flux and equilibrium quality at the MDNBR location as predicted by the ORFEO-HMP CHF correlation. The two data sets provide an equivalent coverage of the test domain. Each partition therefore provides an adequate representation of the range of applicability and is sufficiently large to assess the correlation uncertainty.

Figure 6-2 Distribution of the defining and validation data sets for the ORFEO-HMP correlation (pressure vs. mass flux)

Figure 6-3 Distribution of the defining and validation data sets for the ORFEO-HMP correlation (equilibrium quality vs. pressure)

[ ]

Figure 6-4 Distribution of the defining and validation data sets for the ORFEO-HMP correlation (mass flux vs. equilibrium quality)

The defining data set was evaluated using COBRA-FLX and local thermal-hydraulic conditions were generated for each statepoint (Table B-3). The coefficients in the F_{SPACER} term of the ORFEO-HMP correlation were optimized via successive iterations using the algorithm described in Appendix C of [1] - the same was used for ORFEO-GAIA and ORFEO-NMGRID in [1]. The optimized set of coefficients is listed in Table 6-5. The coefficient optimization process is based on [ ]. Consistent with this approach, the statistical analysis performed in Section 7.1 is based on [ ]

The following can be noted regarding the F_{SPACER} coefficients in Table 6-5:

1. f_0 = f_9=0.0 therefore, F_{GSP} = 1.0 and the value assigned to $l_{grid,2}$ is irrelevant. For the ORFEO-HMP correlation there is no grid spacing impact on the predicted CHF.

2. g_0 = 0.0 therefore,$F_{GUIDE\ TUBE}$ = 1.0 and the valued assigned to rtg is irrelevant. The statistical analysis in Section 7.1 indicates that the unit subchannel and guide tube subchannel CHF performances are statistically distinguishable and this was adequately captured in the design limit calculation.

Table 6-5 Coefficients in F_{SPACER} term for ORFEO-HMP correlation

[ ]

6.4 Correlation behavior

Figure 6-5, Figure 6-6, and Figure 6-7 show the ORFEO-HMP correlation behavior as a function of pressure, mass flux and effective quality, respectively.

Two observations apply to correlation functional behavior. First, there are no discontinuities; second, the functional behavior is consistent with the Groeneveld CHF tables published in [16].

Figure 6-5 Predicted CHF as a function of pressure for ORFEO-HMP correlation

Figure 6-6 Predicted CHF as a function of mass flux for ORFEO-HMP correlation

Figure 6-7 Predicted CHF as a function of effective quality for ORFEO-HMP correlation

7.0 CORRELATION ASSESSMENT AND STATISTICAL ANALYSIS

7.1 ORFEO-HMP CHF correlation with the Pressure-Velocity solver

7.1.1 Analysis of defining and validation data sets

The ORFEO-HMP CHF correlation has been developed based on the defining data set described in Section 6.3. The validation data set represents a second set of experimental data that is used to confirm the adequacy of the correlation using data that was not used to fit the correlation.

The validation data set must be confirmed to be poolable with the defining data set, i.e. the correlation should predict the validation data set with approximately the same level of accuracy as the defining data set.

Poolability was checked by performing the following statistical tests:

- F-test (verifies the homogeneity of variances between the two data sets)
- Two-sample t-test (verifies the equality of means between the two data sets)

A prerequisite for these tests is that the population is normally distributed. The normality was checked by applying the Anderson-Darling test. The null hypothesis for the test states that the data set is normally distributed. However, it is well known in the open literature and stated in NUREG/CR-4604 ([17], pg. 535) that large data sets often provide false indications that the data sets are not normally distributed due to the statistical tests becoming overly sensitive with increasing data set size. As an alternative to normality tests, the data can be visually verified to be normally distributed by comparison of the data histogram with a normal (Gaussian) curve.

The tests are used at a 5% significance level. The results of these tests are shown in Table 7-1. [ ] Figure 7-1 shows the histograms of the M/P populations for the defining and validation data sets with the normal distribution curve. [

]

Table 7-1 Results of statistical tests applied to the defining and validation data sets for ORFEO-HMP correlation

[ ]

Figure 7-1 Histogram of M/P for the defining and validation data sets for ORFEO-HMP correlation

[ ]

Table 7-2 compares the statistics for each test campaign. The average M/P and standard deviation values of the defining and validation data sets for each test are reasonably close such that there is no difference in the predictive behavior of the correlation. Any differences are small relative to the experimental uncertainty. Based on the results of tests for homogeneity of variances and equality of means it is concluded that the defining and validation data sets are poolable. Therefore, the correlation adequately describes the statepoints in the validation data set.

Table 7-2 Overall statistics of the defining and validation data sets for the ORFEO-HMP correlation

Figure 7-2, Figure 7-3, and Figure 7-4 show the distribution of the M/P data as a function of pressure, mass flux, and equilibrium quality. These figures illustrate that the ORFEO-HMP correlation adequately describes the two data sets.

Figure 7-2 M/P versus pressure for ORFEO-HMP correlation (defining and validation data sets)

Figure 7-3 M/P versus mass flux for ORFEO-HMP correlation (defining and validation data sets)

[ ]

Figure 7-4 M/P versus equilibrium quality for ORFEO-HMP correlation (defining and validation data sets)

[

]

Since M/P values for the defining and validation data sets were found to be poolable, they were combined together into one data set. The CHF tests used exclusively for validation (see Table 6-3 and Table 6-4) are also added. The resulting data set, which is referred to as the "combined" data set, comprises 7507 data points and it is used for the statistical design limit calculation. The statistics of the combined data set are shown in Table 7-3.

Table 7-3 Overall statistics of the combined data set for the ORFEO-HMP correlation with the Pressure-Velocity solver

Table 7-3 Overall statistics of the combined data set for the ORFEO-HMP correlation with the Pressure-Velocity solver (continued)

[ ]

Table 7-3 Overall statistics of the combined data set for the ORFEO-HMP correlation with the Pressure-Velocity solver (continued)

Table 7-3 Overall statistics of the combined data set for the ORFEO-HMP correlation with the Pressure-Velocity solver (continued)

[ ]

Figure 7-5 shows the histogram of the M/P population obtained when evaluating the combined data set with the ORFEO-HMP correlation. A normal distribution provides a good approximation of the M/P distribution.

Figure 7-5 Histogram of the combined data set for the ORFEO-HMP correlation

[ ]

7.1.2 Design limit

The design limit of the ORFEO-HMP correlation is calculated using Owen's methodology [18]; the same was used for ORFEO-GAIA and ORFEO-NMGRID in [1].

The design limit is calculated based on the combined CHF test data set listed in Table 7-3. The values of the main parameters of the design limit calculation are listed in Table 7-4. When using the standard deviation of [ ] which is based on the total variance of the M/P population, the resulting design limit is [ ]. The correlation design limit has to ensure that all sub-regions are adequately protected such that there are no non-conservative sub-regions. The acceptability of this value is confirmed by investigating the distribution of the statepoints that have an M/P lower than the inverse of the design limit in each pressure, mass flux and equilibrium quality sub-region, and in each CHF test.

The results show [ ] statepoints below the design limit with the majority of these distributed as follows:

- in CHF tests K2200/1/2, K2402, K3100, K3200, K3800, K9200, K9300, and SP400
- at pressures between 0 and 53 bar and between 66 bar and 90 bar
- at mass fluxes between 0 and 1600 kg/m^{2}s
- at equilibrium qualities between 0.25 and 1.0

Based on the number and distribution of statepoints below the design limit, non-conservative sub-regions may exist in these ranges. Therefore the design limit is recalculated using a more limiting standard deviation that bounds all sub-regions and CHF tests (Table 7-3, Table 7-5, Table 7-6 and Table 7-7) instead of the standard deviation based on the total variance of the combined

data set. This value [ ] is termed the "bounding standard deviation" in Table 7-4. The resulting correlation design limit is [ ].

Table 7-5, Table 7-6 and Table 7-7 show the distribution of the statepoints that have an M/P value lower than the inverse of the design limit between the pressure, mass flux and equilibrium quality ranges. No individual range or CHF test exhibits an unexpected number of statepoints below the inverse of the design limit. The acceptability of the [ ] design limit is further confirmed by investigating the distribution of the statepoints that have an M/P lower than the inverse of the design limit using the method described in [19]. Pressure, mass flux and equilibrium quality are binned together all three at once and concluded to exhibit an acceptable number of data points below the inverse of the design limit for each bin.

Table 7-4 Statistical parameters and design limit for ORFEO-HMP correlation [ ]

[ ]

Table 7-5 Distribution of statepoints below the ORFEO-HMP correlation design limit by pressure ranges

[ ]

Table 7-6 Distribution of statepoints below the ORFEO-HMP correlation design limit by mass flux ranges

[ ]

Table 7-7 Distribution of statepoints below the ORFEO-HMP correlation design limit by equilibrium quality ranges

[ ]

The combined data set of the ORFEO-HMP correlation is further investigated based on the geometric characteristics of the test assemblies. Table 7-8, Table 7-9, Table 7-10, Table 7-11, and Table 7-12 show the mean and standard deviation values of the M/P population based on grid design, fuel assembly design, subchannel, axial power profile, and axial configuration. For the groups in "fuel assembly design " an ANOVA was performed to verify the equality of means. For the groups in "grid design", "subchannel", "axial power profile", and "axial configuration" a two-sample t-test was performed to verify the equality of means. The ANOVA and t-test are used at a 5% significance level. A test for homogeneity of variances is not necessary since the ANOVA and the t-test account for non-equal variances. The statistical analysis results are shown in Table 7-13 and indicate that biases, although small, exist between the groups in each category; therefore the design limit of ORFEO-HMP should be based on the most limiting group. This is the same as verifying that the design limit adequately bounds each group in each category, which is done below.

The design limit of [ ] (Table 7-4) has to ensure that, for each group, all sub-regions are adequately protected such that there are no non-conservative sub-regions. The acceptability of this value is confirmed by investigating the distribution of the statepoints that have an M/P lower than the inverse of the design limit in each pressure, mass flux and equilibrium quality sub-region for each group. For the IFM group, the 37-53 bar pressure subregion, the 500-900 kg/m^{2}s mass flux subregion and the 0.4-0.6 quality subregion, each has the ratio of the non-conservative statepoints relative to the total number of statepoints greater than 5%. The distribution of the non-conservative statepoints in each sub-region is further investigated using the method described in [19]. The results indicate that no non-conservative sub-regions exist.

The existence of potentially non-conservative sub-regions, for each group, is further investigated by binning pressure, mass flux and equilibrium quality together, all three at once. The total number of statepoints and the number of statepoints with an M/P below the inverse of design limit ([ ])

in each bin is determined. The results indicate that the regions listed in Table 7-14 are potentially non-conservative. The increase of the design limit to [ ] produces the results shown in Table 7-14 where all the sub-regions are adequately protected. The parameters of the design limit calculation are shown in Table 7-15.

Table 7-8 Overall statistics of the combined data set for the ORFEO-HMP correlation by grid design type

[ ]

Table 7-9 Overall statistics of the combined data set for the ORFEO-HMP correlation by fuel assembly design

[ ]

Table 7-10 Overall statistics of the combined data set for the ORFEO-HMP correlation by subchannel type

[ ]

Table 7-11 Overall statistics of the combined data set for the ORFEO-HMP correlation by axial power profile type

[ ]

Table 7-12 Overall statistics of the combined data set for the ORFEO-HMP correlation by axial configuration type

[ ]

Table 7-13 Results of statistical tests applied to ORFEO-HMP combined data set (grid design, fuel assembly, subchannel, axial power profile, and axial configuration)

[ ]

Table 7-14 Potentially non-conservative subregions [ ]

[ ]

Table 7-15 Statistical parameters and design limit for ORFEO-HMP correlation [ ]

[ ]

Trends that can potentially impact the prediction capability of the ORFEO-HMP correlation are investigated by reviewing the plots of M/P as a function of pressure, mass flux, equilibrium quality and burnout length for each group in “grid design”, “fuel assembly design”, “subchannel”, “axial power profile”, and “axial configuration”. The trends in quality are particularly important because the correlation behavior at low equilibrium quality is based on extension of measured CHF performance at higher qualities. Statepoints at qualities below approximately -10% are difficult to measure experimentally; however, CHF prediction capability in this range is required by safety analysis applications. Therefore, the correlation predictions are extended in these regions.

[ ]

Figure 7-6 Prediction interval for M/P versus quality for 14x14 and 16x16 fuel assembly design

Figure 7-7 through Figure 7-15 show the M/P data as a function of pressure, mass flux, equilibrium quality, burnout length, distance-to-grid, grid spacing, rod pitch, rod diameter, and guide tube diameter, respectively. The design limit adequately bounds the combined data set.

Figure 7-7 M/P versus pressure for ORFEO-HMP correlation (combined data set)

Figure 7-8 M/P versus mass flux for ORFEO-HMP correlation (combined data set)

Figure 7-9 M/P versus equilibrium quality for ORFEO-HMP correlation (combined data set)

Figure 7-10 M/P versus burnout length for ORFEO-HMP correlation (combined data set)

[

]

Figure 7-11 M/P versus distance-to-grid for ORFEO-HMP correlation (combined data set)

Figure 7-12 M/P versus grid spacing for ORFEO-HMP correlation (combined data set)

Figure 7-13 M/P versus rod pitch for ORFEO-HMP correlation (combined data set)

Figure 7-14 M/P versus rod diameter for ORFEO-HMP correlation (combined data set)

[ ]

Figure 7-15 M/P versus guide tube diameter for ORFEO-HMP correlation (combined data set)

[

]

7.1.3 Low quality extension

The equilibrium quality range required for CHF correlation use in applications cannot be covered in its entirety in CHF testing with rod assemblies. Specifically, equilibrium qualities below -10% are difficult to achieve in CHF testing however, they are quite common in DNB licensing analyses. Therefore, the applicability of an unbounded lower quality limit for ORFEO-HMP needs to be demonstrated. The same process used to justify unbounded lower quality limits for ORFEO-GAIA and ORFEO-NMGRID in the response to RAI-SNPB-12 [1] is employed here.

The justification is based on evaluation of the available [ ] with ORFEO-HMP (the same data was used in [1]). Figure 7-16, Figure 7-17, and Figure 7-18 show the distribution of the [ ] relative to the ORFEO-HMP data set. The two sets of data overlap in pressure and mass flux but in terms of equilibrium quality the [ ] while the ORFEO-HMP data set does not go below -13% (exception being one isolated statepoint around -25%).

Figure 7-16 ORFEO-HMP and [ ] sets (pressure vs. mass flux)

[ ]

Figure 7-17 ORFEO-HMP and [ ] sets (mass flux vs. equilibrium quality)

Figure 7-18 ORFEO-HMP and [ ] sets (equilibrium quality vs. pressure)

[

]

The [ ] is evaluated with the ORFEO-HMP correlation. The M/P values for the [ ] set are plotted together with the M/P values of the ORFEO-HMP data set as a function of pressure, mass flux and equilibrium quality in Figure 7-19, Figure 7-20, and Figure 7-21. [ ] However, the application of the correlation to low qualities is subject to the limitation resulting from the trend analysis, which is -60% lower bound on quality.

Figure 7-19 M/P versus pressure (ORFEO-HMP data set vs. [ ] set)

Figure 7-20 M/P versus mass flux (ORFEO-HMP data set vs. [ ] set)

[

]

Figure 7-21 M/P versus equilibrium quality (ORFEO-HMP data set vs. [ ] set)

7.1.4 Validation of application to [ ]

The maximum value for the grid spacing in the combined data set is [ ] and this covers the application needs. However, the maximum value for [ ]. In this section, the ORFEO-HMP correlation is validated for application to [ ].

The review of the ORFEO-HMP correlation form (Section 6.2) and coefficients (Section 6.3) indicates that $F_{GRID} \neq 0$ therefore, the predicted CHF is a function of [ ]. Figure 7-11 illustrates [ ]

The magnitude of [ ] effect on the predicted CHF is investigated. Calculations performed on ORFEO-HMP for various statepoints indicated that the predicted CHF performance [ ]. Figure 7-22 shows the relative variation in predicted CHF for [ ] Based on the evaluation above it can be concluded that:

[ ]

Figure 7-22 Relative difference in CHF predicted by ORFEO-HMP as a function of [ ]

[ ]

7.1.5 Application range

The application range for the ORFEO-HMP correlation is established based on the coverage of the CHF test data set in terms of pressure, mass flux and equilibrium quality. The CHF tests are designed to cover the parameter ranges required by safety analysis applications. Figure 7-23, Figure 7-24, and Figure 7-25 show the distribution of the combined data set in terms of pressure, mass flux, and equilibrium quality at the MDNBR location as predicted by the ORFEO-HMP correlation.

The application range (local thermal-hydraulic conditions) for the ORFEO-HMP CHF correlation is listed in Table 7-16.

Figure 7-23 Distribution of the combined data set for the ORFEO-HMP correlation (pressure vs. mass flux)

[ ]

Figure 7-24 Distribution of the combined data set for the ORFEO-HMP correlation (mass flux vs. equilibrium quality)

Figure 7-25 Distribution of the combined data set for the ORFEO-HMP correlation (equilibrium quality vs. pressure)

[ ]

Table 7-16 Range of application for ORFEO-HMP correlation with the Pressure-Velocity solver (local thermal-hydraulic conditions)

Parameter	Units	Minimum value	Maximum value
Pressure	bar	19.5	179.6
	psia	282.8	2604.9
Mass flux	kg/m^2s	235.0	4650.0
	$Mlbm/ft^2hr$	0.1733	3.4286
Equilibrium quality	fraction	-0.6	0.8792

7.1.6 Impact of the test facility heat loss

[ ]

Table 7-17 Statistical parameters and design limit for ORFEO-HMP correlation [ ]

[ ]

7.2 ORFEO-HMP CHF correlation with the SCHEME-Pressure solver

In Section 7.1, the ORFEO-HMP correlation was developed and validated using the Pressure-Velocity solver in COBRA-FLX. In this section, the ORFEO-HMP correlation is validated for use with the SCHEME-Pressure solver. The statistics of the combined data set are shown in Table 7-18. The design limit was calculated by applying the same method used in Section 7.1.2 for the Pressure-Velocity solver. The parameters of the design limit calculation are shown in Table 7-19. It was verified that the design limit of [ ] (the same as for the Pressure-Velocity solver) adequately protects all tests and subregions when used with the SCHEME-Pressure solver.

An analysis is performed to demonstrate that, for each group in each category (HTP grid, non-mixing grid, 14x14 fuel assembly design, etc.) the differences between the data sets generated using the Pressure-Velocity solver and the SCHEME-Pressure solver are insignificant. The results indicate that the data sets are statistically indistinguishable. Therefore, in regards with the biases and trends analyses, the results obtained with the Pressure-Velocity solver are applicable to the SCHEME-Pressure solver.

The application range for the ORFEO-HMP correlation used with the SCHEME-Pressure solver is established. The same method and type of limitations used in Section 7.1.5 are applied. The application range in terms of local thermal-hydraulic conditions is listed in Table 7-20. There is no change in application range for the fuel assembly geometry.

The design limit is adjusted to account for the impact of the test facility heat loss. The same method used for the ORFEO-HMP correlation with the Pressure-Velocity solver is applied. The resulting design limit for use with the SCHEME-Pressure solver is [ ] (Table 7-21).

Table 7-18 Overall statistics of the combined data set for the ORFEO-HMP correlation with the SCHEME-Pressure solver

[ ]

Table 7-18 Overall statistics of the combined data set for the ORFEO-HMP correlation with the SCHEME-Pressure solver (continued)

[

]

Table 7-18 Overall statistics of the combined data set for the ORFEO-HMP correlation with the SCHEME-Pressure solver (continued)

Table 7-18 Overall statistics of the combined data set for the ORFEO-HMP correlation with the SCHEME-Pressure solver (continued)

[ ]

Table 7-19 Statistical parameters and design limit for ORFEO-HMP correlation with the SCHEME-Pressure solver [ ]

[ ]

Table 7-20 Range of application for ORFEO-HMP CHF correlation with the SCHEME-Pressure solver (local thermal-hydraulic conditions)

Parameter	Units	Minimum value	Maximum value
Pressure	bar	19.5	179.6
	psia	282.8	2604.9
Mass flux	kg/m^2s	248.7	4650.0
	$Mlbm/ft^2hr$	0.1834	3.4286
Equilibrium quality	fraction	-0.6	0.8769

Table 7-21 Statistical parameters and design limit for ORFEO-HMP correlation with the SCHEME-Pressure solver [ ]

[ ]

8.0 QUALITY ASSURANCE PROGRAM (QAP)

8.1 QAP specific to correlation development

The ORFEO-HMP correlation is developed and maintained under a quality assurance program that meets the regulatory requirements of 10 CFR Part 50 Appendix B.

8.2 QAP specific to CHF testing

The testing organization (that operates the KATHY loop) is treated as a supplier for testing and data that is subject to 10 CFR Part 50 Appendix B. As such, periodic audits are performed on the quality assurance program of the supplier to ensure that it remains in compliance with the quality assurance requirements. The frequency of the audits is based on the compliance history of the supplier and the frequency of use of the supplier. Certification of the supplier is provided for a specified period of time.

9.0 REFERENCES

1. "The ORFEO-GAIA and ORFEO-NMGRID Critical Heat Flux Correlations", ANP-10341P-A, Rev. 0, Framatome Inc., September 2018
2. Standard Review Plan for the Review of Safety Analysis Reports for Nuclear Plants: LWR Edition, NUREG-0800, March 2007
3. R. H. Wilson, D. A. Farnsworth and R. H. Stoudt, "BWC Correlation of Critical Heat Flux", BAW-10143P-A, Babcock & Wilcox, April 1985
4. D. A. Farnsworth and G. A. Meyer, "The BWU Critical Heat Flux Correlations", BAW-10199P-A, Rev. 0, Framatome Technologies, February 1998
5. D. A. Farnsworth and R. L. Harne, "BHTP DNB Correlation Applied with LYNXT", BAW-10241(P)(A), Rev. 2, Framatome ANP, Inc., September 2020
6. D. A. Farnsworth and R. L. Harne, "The ACH-2 CHF Correlation for the U.S. EPR", ANP-10269P-A, Rev. 0, AREVA NP Inc., December 2007
7. WCAP-15306-NP-A Addendum 2 Revision 0, "Extended Application of ABB-NV Correlation and Modified ABB-NV Correlation WLOP for PWR Low Pressure Applications", September 2006
8. CENPD-387-NP-A Revision 000, "ABB Critical Heat Flux Correlations for PWR Fuel", CE Nuclear Power LLC, May 2000
9. TR-0116-21012-NP Rev. 0, "NuScale Power Critical Heat Flux Correlation NSP2"
10. "COBRA-FLX: A Core Thermal-Hydraulic Analysis Code", ANP-10311P-A, Revision 1, Framatome Inc., October 2017

11. J. G. Collier and J. R. Thome, "Convective Boiling and Condensation", 3rd Edition, Clarendon Press, Oxford, May 1994

12. C. F. Fighetti and D. G. Reddy, "Parametric Study of CHF Data, Volume 2: A Generalized Subchannel CHF Correlation for PWR and BWR Fuel Assemblies", NP-2609, Volume 2, EPRI, January 1983

13. D.C. Groeneveld, J.Q. Shan, A.Z. Vasic, L.K.H. Leung, A. Durmayaz, J. Yang, S.C. Cheng and A. Tanase, "The 2006 CHF Look-up Table", Nuclear Engineering and Design 237 (2007) 1909-1922

14. M. Lee, "A Critical Heat Flux Approach for Square Rod Bundles Using the 1995 Groeneveld CHF Table and Bundle Data of Heat Transfer Research Facility", Nuclear Engineering and Design 197 (2000) 357-374

15. L. S. Tong and Y. S. Tang, "Boiling Heat Transfer and Two-Phase Flow", 3rd Edition, Taylor and Francis, 2003

16. D.C. Groeneveld et al., "The 1996 look-up table for critical heat flux in tubes", Nuclear Engineering and Design 163 (1996) 1-23

17. Statistical Methods for Nuclear Material Management, NUREG/CR-4604, December 1988

18. D.B. Owen, "Factors for One-sided Tolerance Limits and for Variable Sampling Plans", SCR-607, Sandia Corporation, March 1963

19. J. Kaizer, "Identification of Nonconservative Subregions in Empirical Models Demonstrated Using Critical Heat Flux Models ", Nuclear Technology, Vol. 190, 2015

Appendix A: Axial Geometry of Test Assemblies

Figure A-1 Axial geometry of CHF test AR15

[ ]

Figure A-2 Axial geometry of CHF test AR16

[ ]

Figure A-3 Axial geometry of CHF test CE090

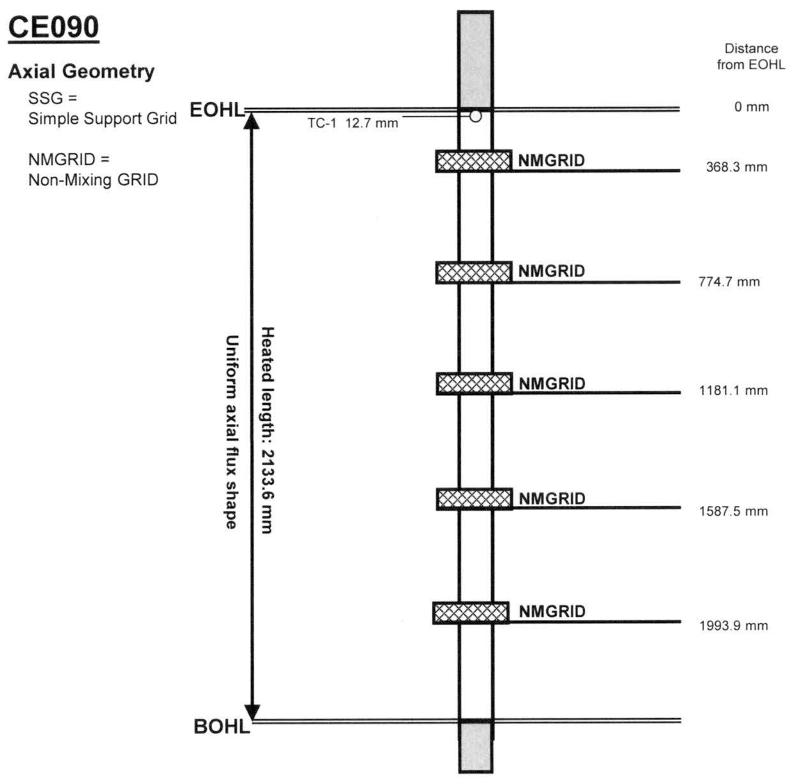

Figure A-4 Axial geometry of CHF test CE100

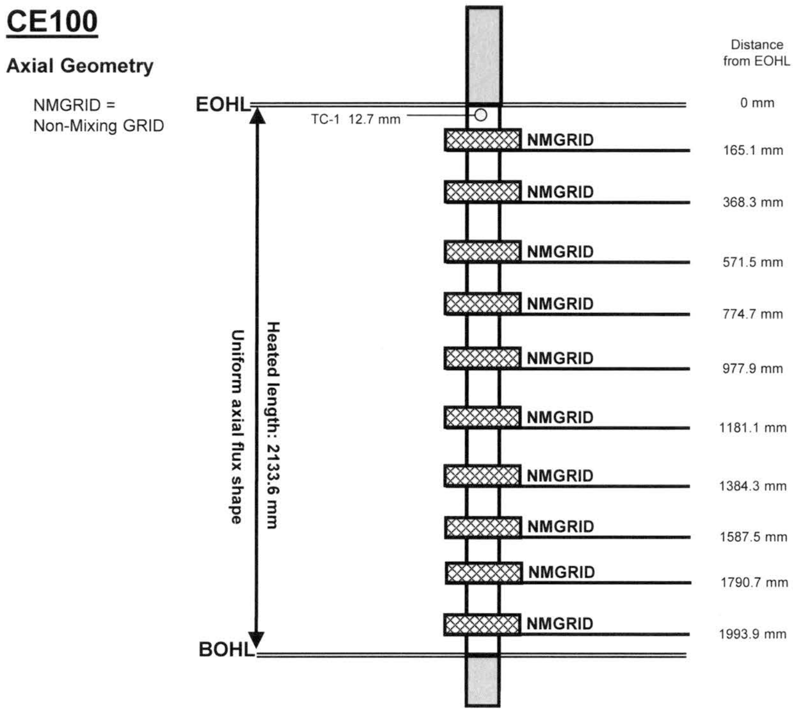

Figure A-5 Axial geometry of CHF test CE130

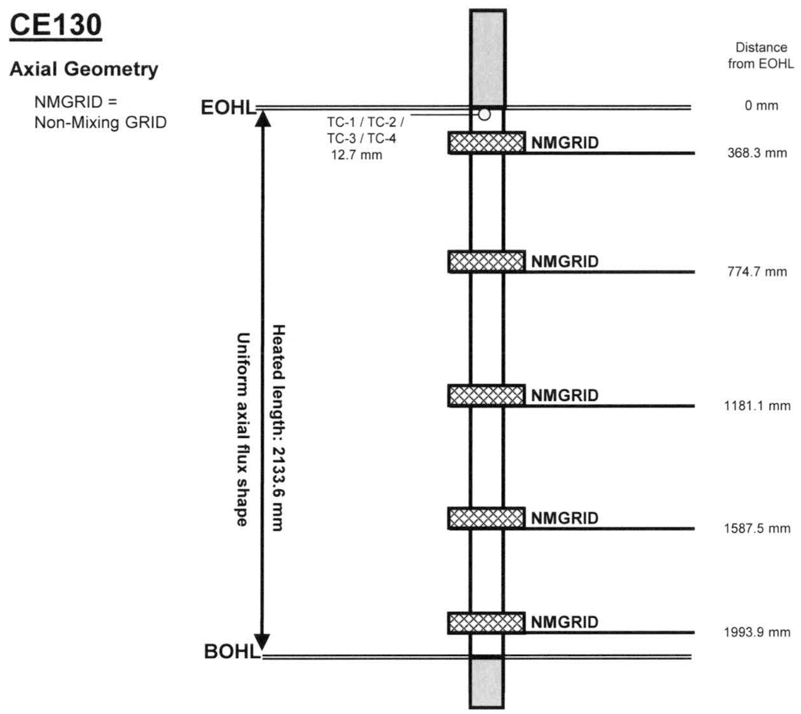

Figure A-6 Axial geometry of CHF test CE180

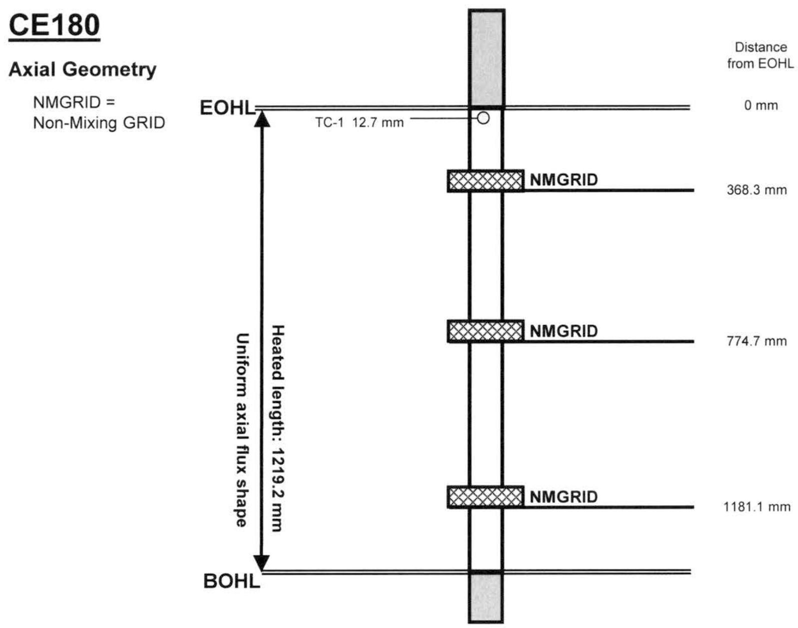

Figure A-7 Axial geometry of CHF test CE190

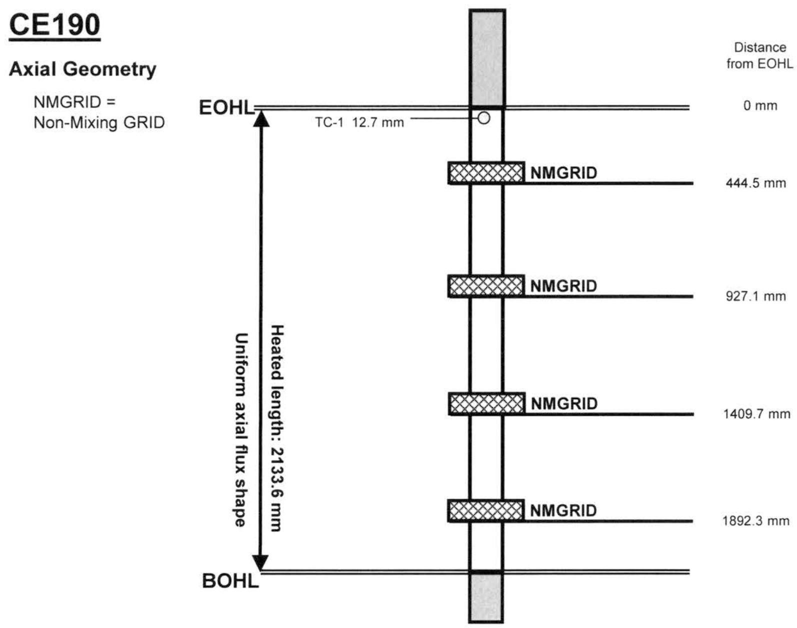

Figure A-8 Axial geometry of CHF test CE210

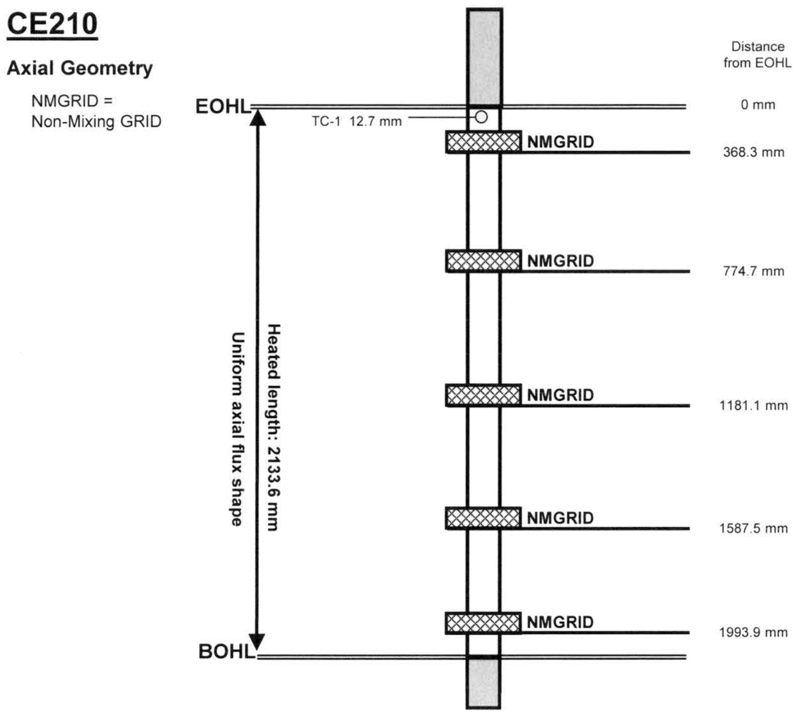

Figure A-9 Axial geometry of CHF test CE290

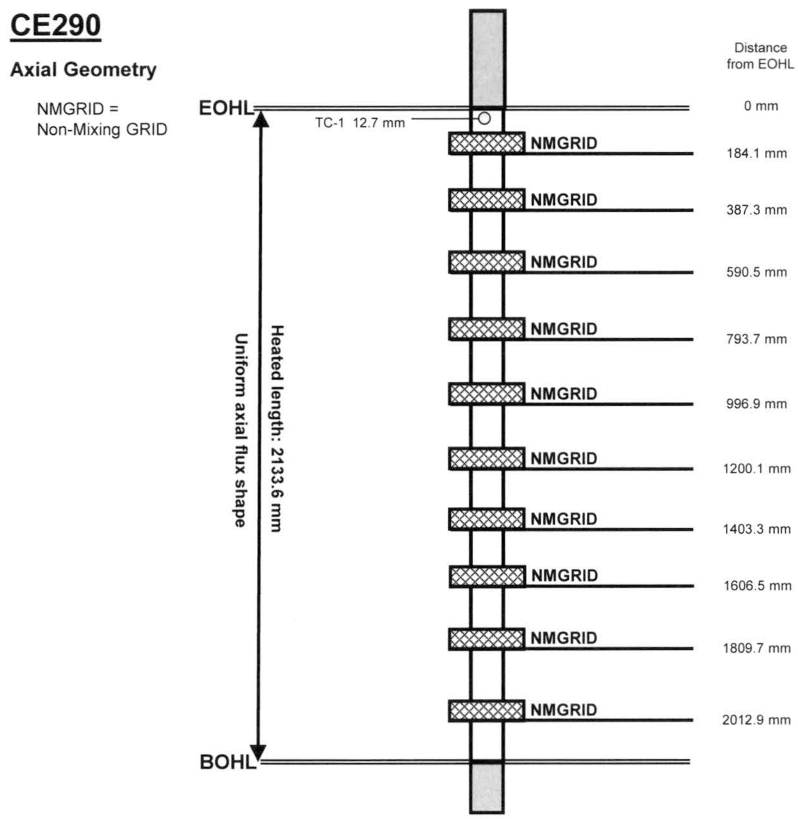

Figure A-10 Axial geometry of CHF test CE300

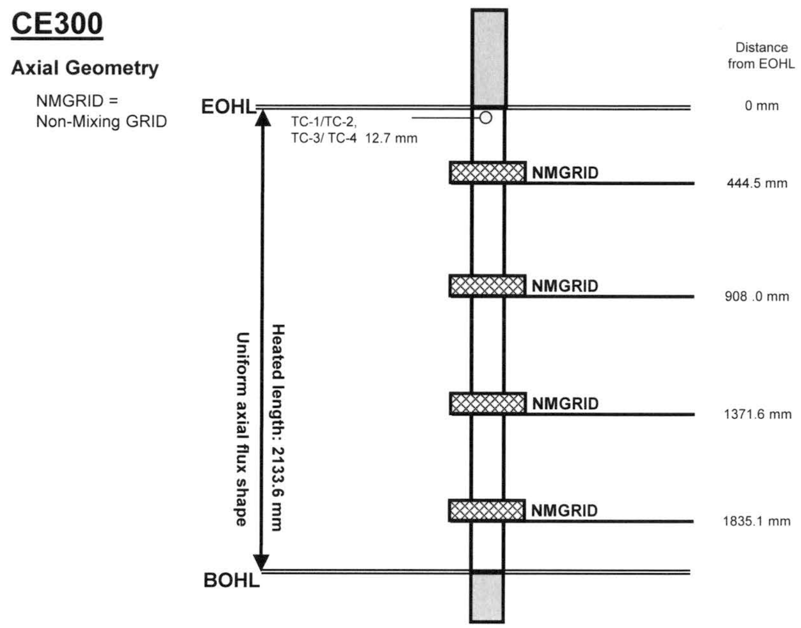

Figure A-11 Axial geometry of CHF test CE330

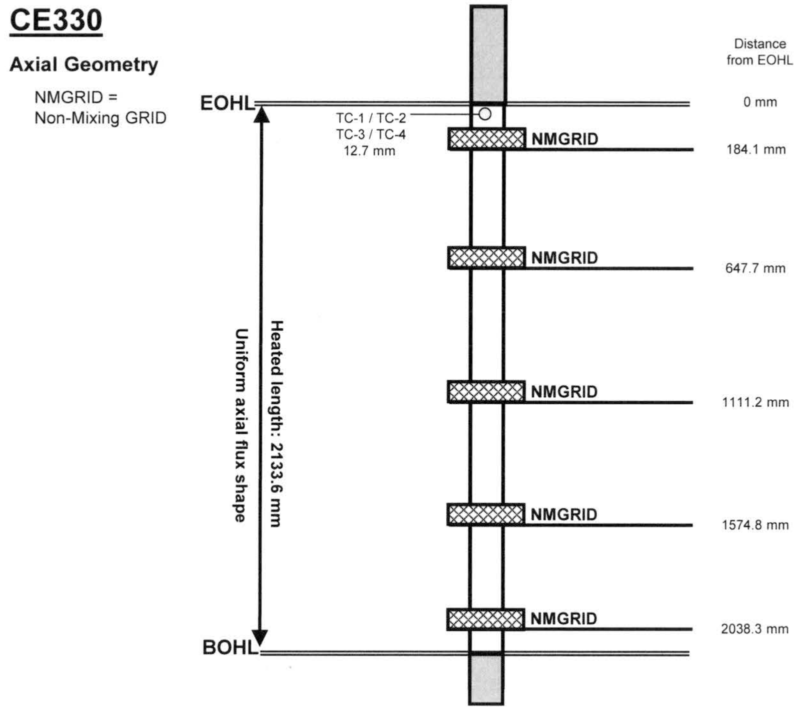

Figure A-12 Axial geometry of CHF test CE360/CE361

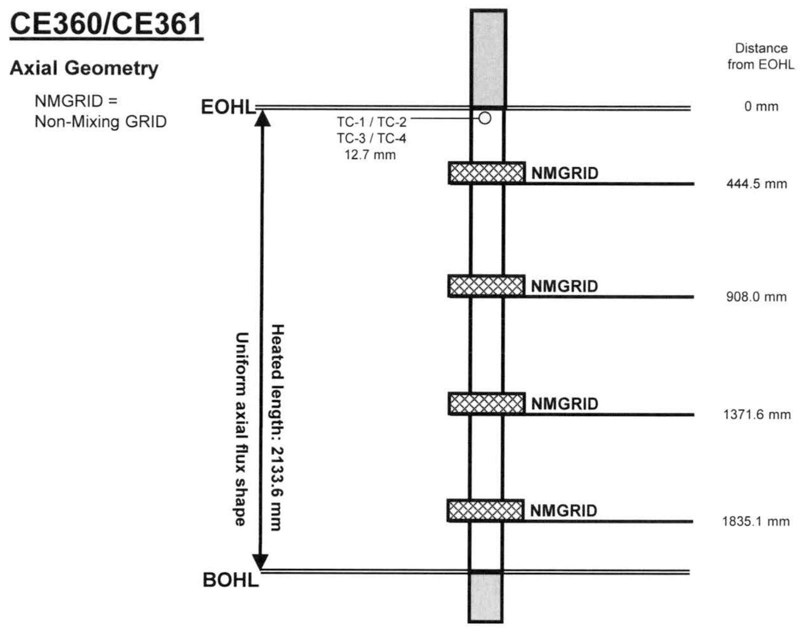

Figure A-13 Axial geometry of CHF test CE370

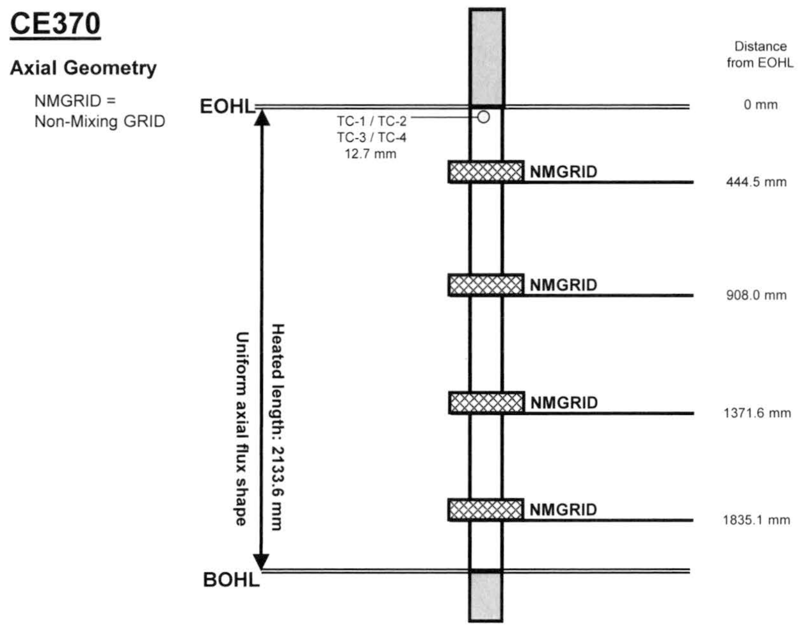

Figure A-14 Axial geometry of CHF test CE380

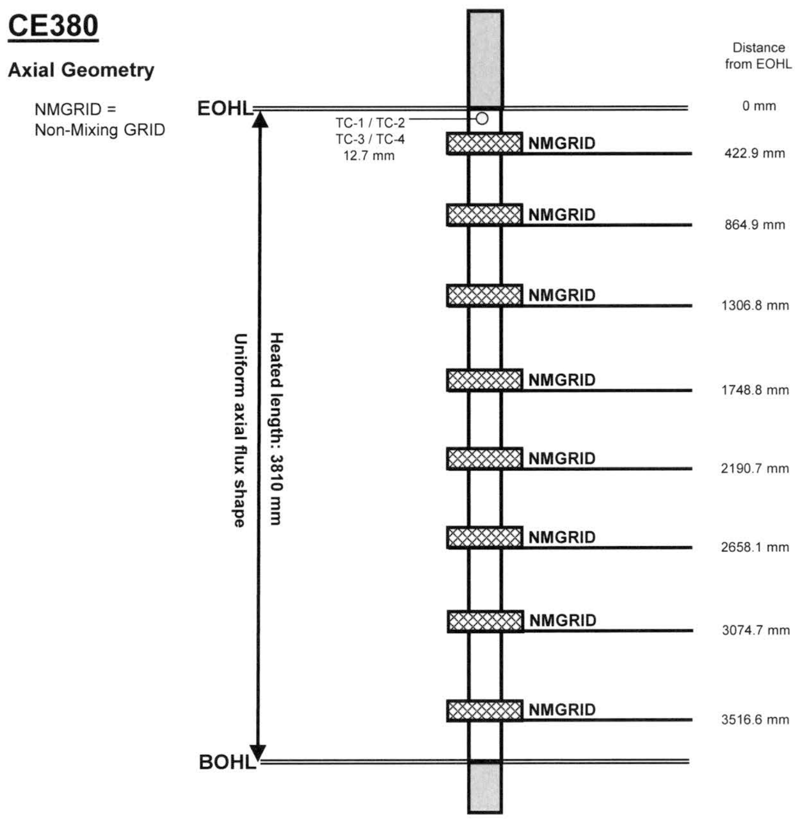

Figure A-15 Axial geometry of CHF test CE410

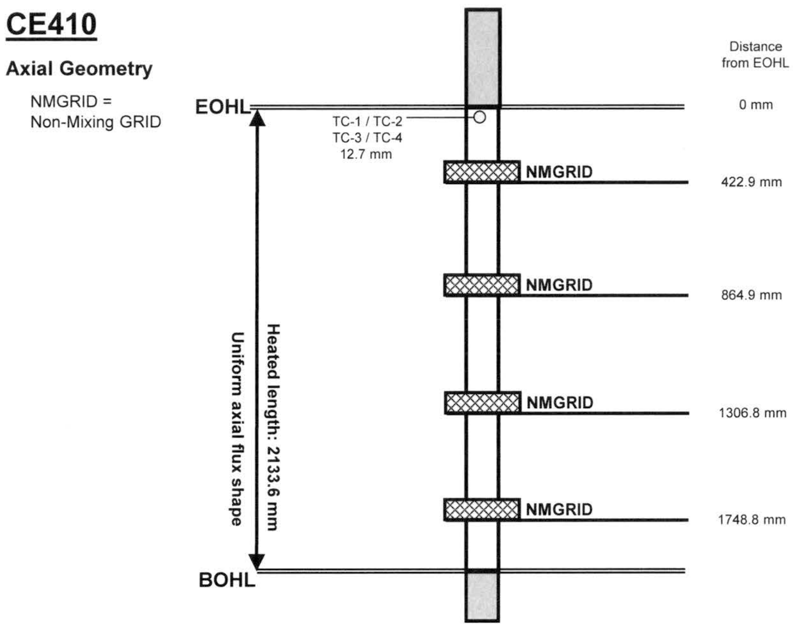

Figure A-16 Axial geometry of CHF test CE420

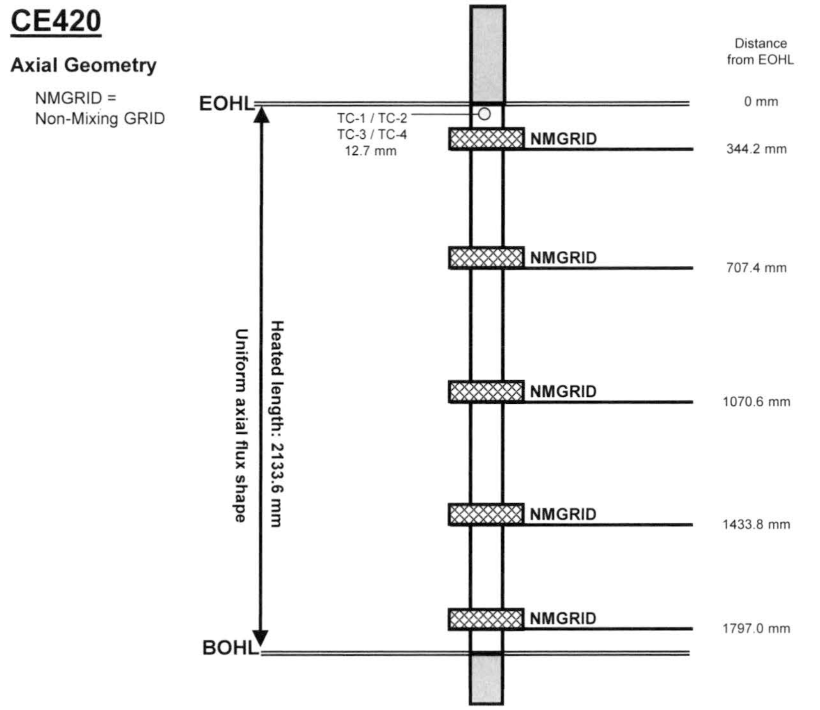

Figure A-17 Axial geometry of CHF test CE430

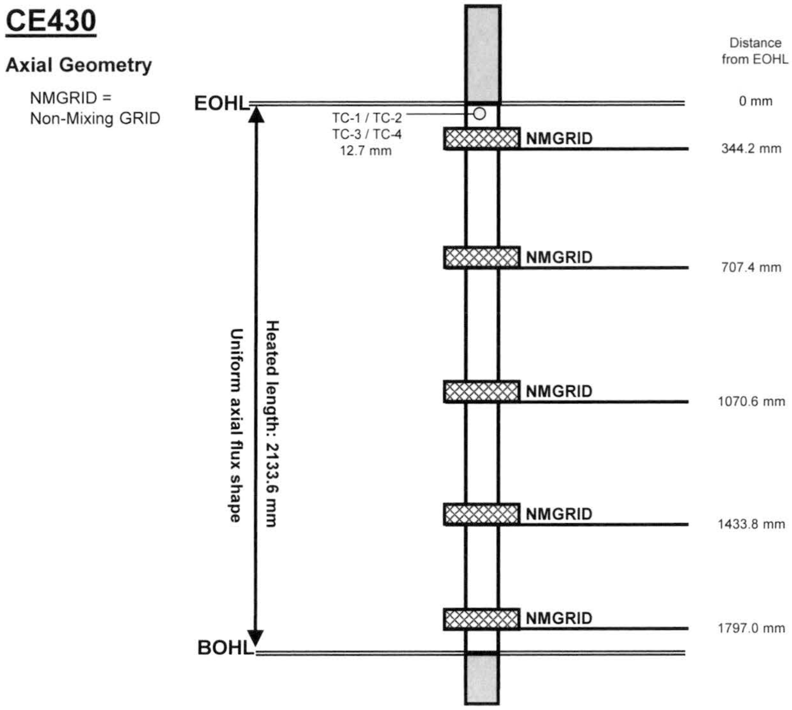

Figure A-18 Axial geometry of CHF test CE470

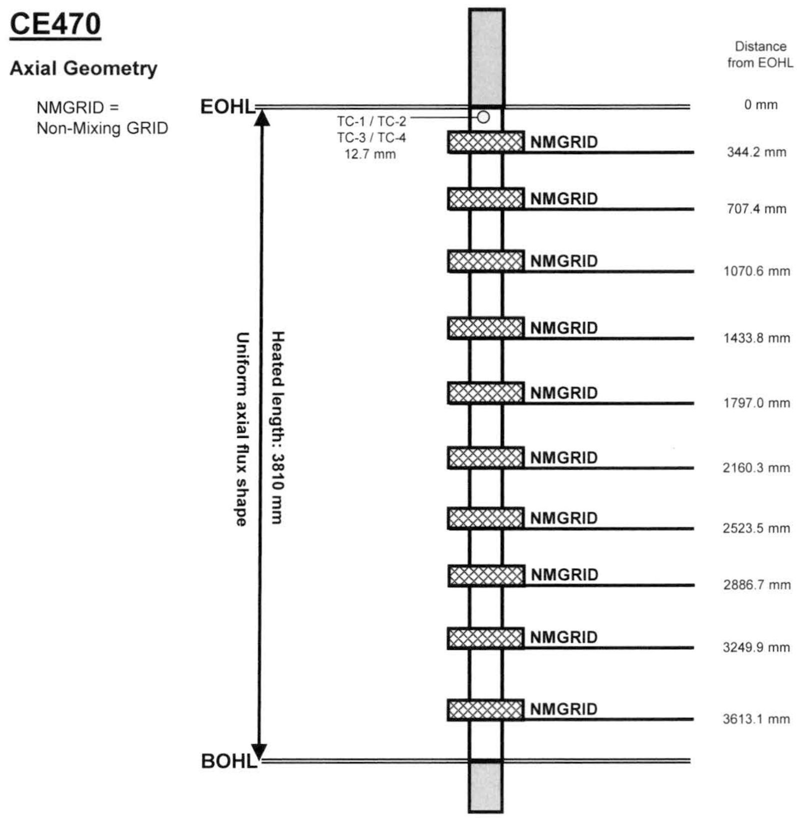

Figure A-19 Axial geometry of CHF test CE480

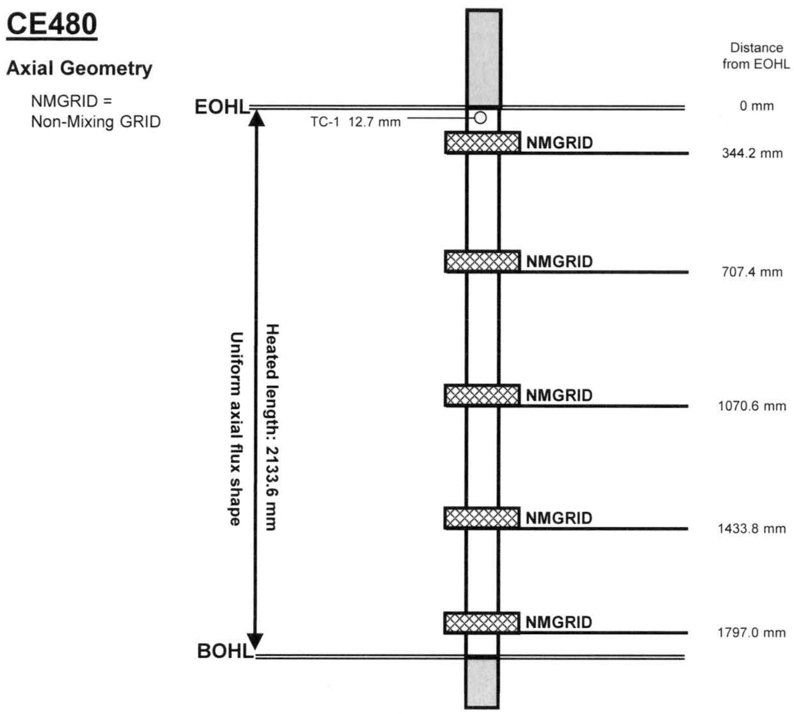

Figure A-20 Axial geometry of CHF test CE520/CE521

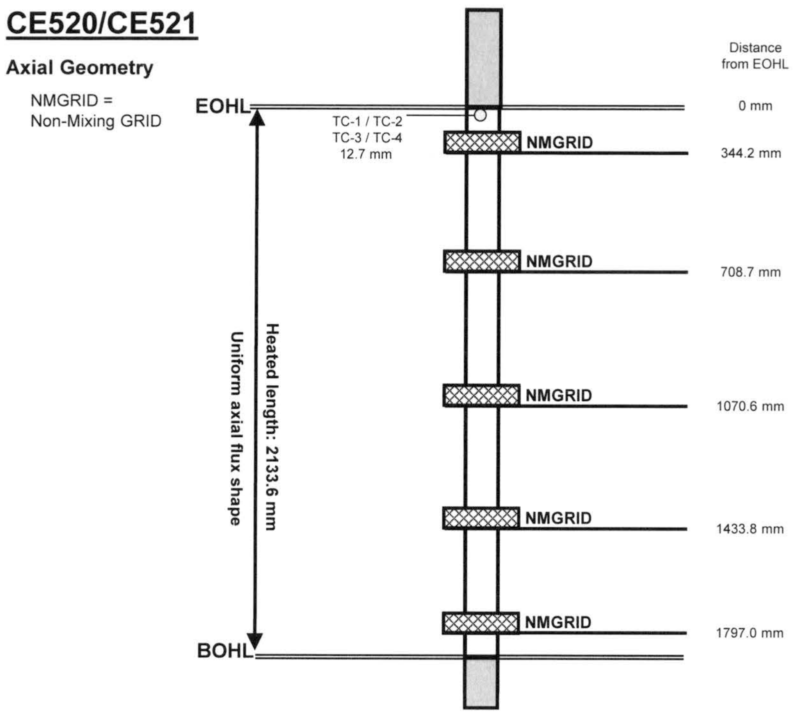

Figure A-21 Axial geometry of CHF test CE580

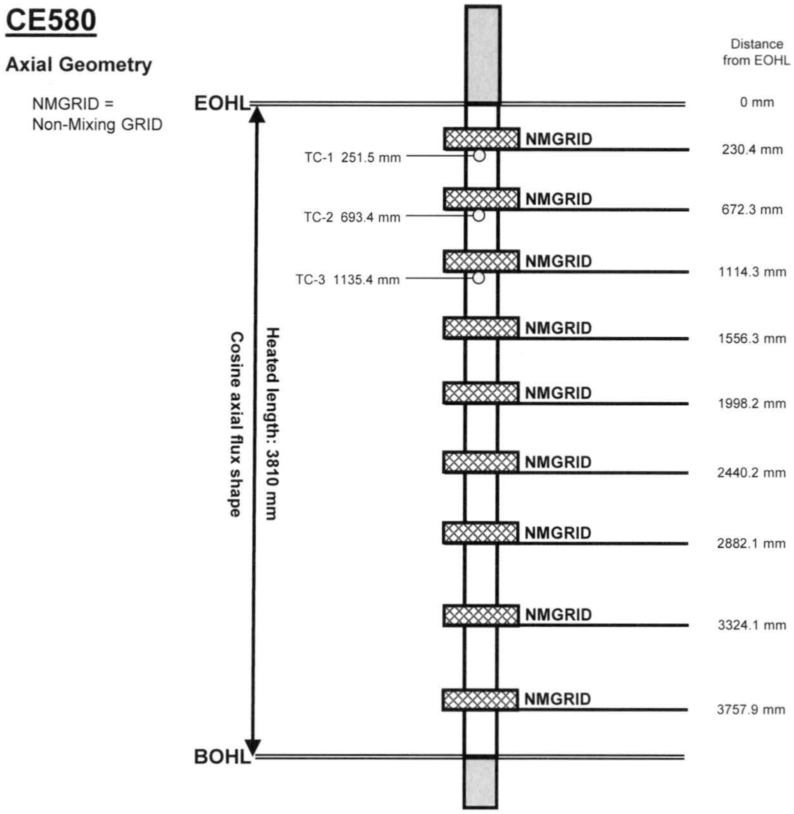

Figure A-22 Axial geometry of CHF test CE590

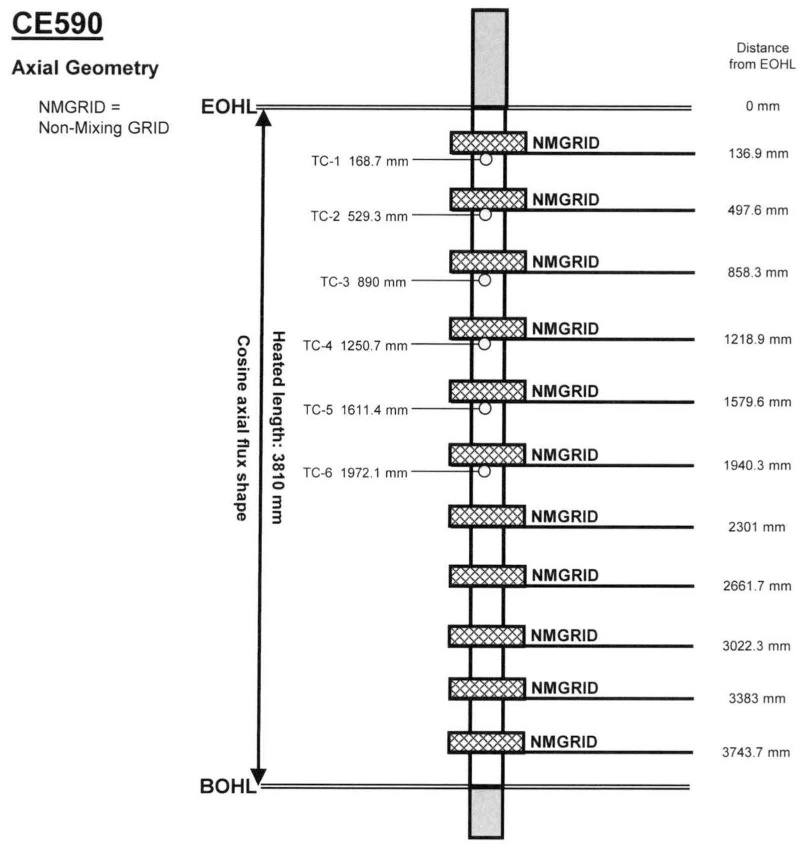

Figure A-23 Axial geometry of CHF test CE600

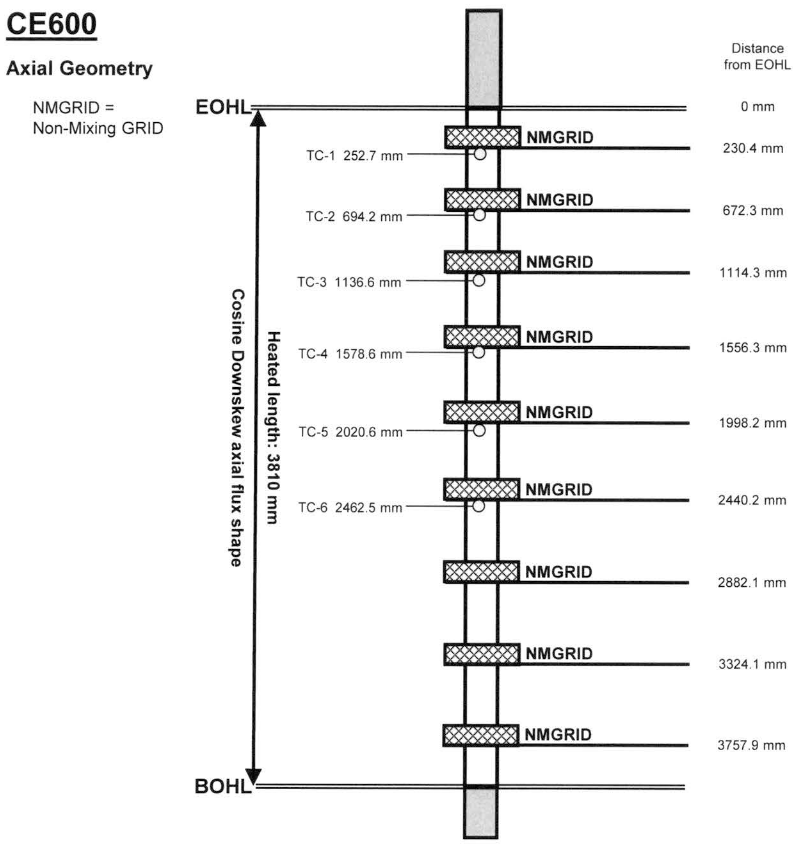

Figure A-24 Axial geometry of CHF test CE660

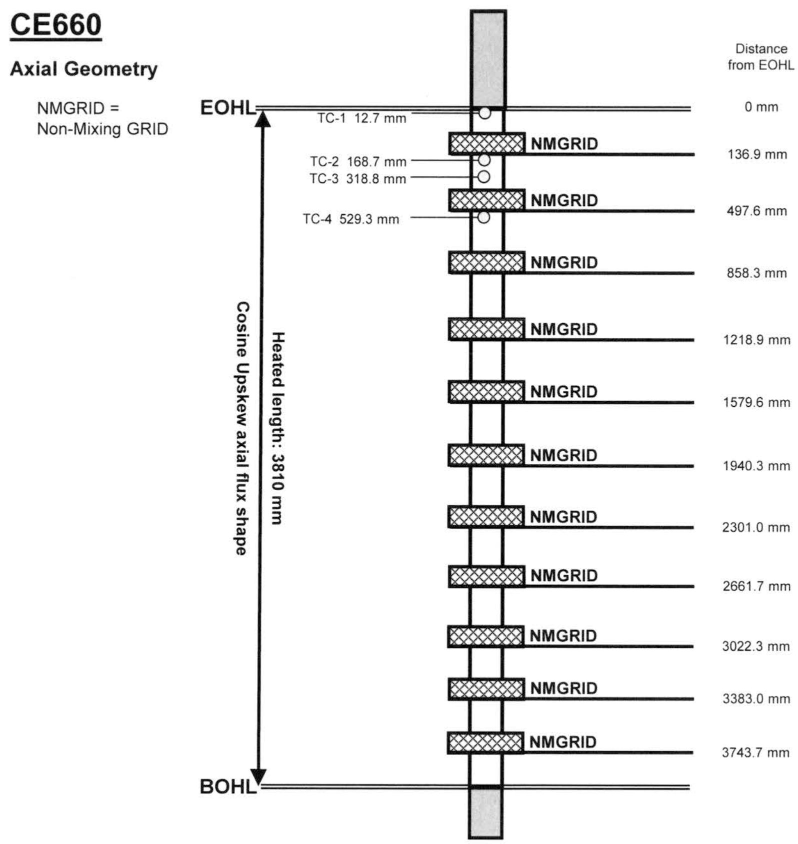

Figure A-25 Axial geometry of CHF test EX201/EX202

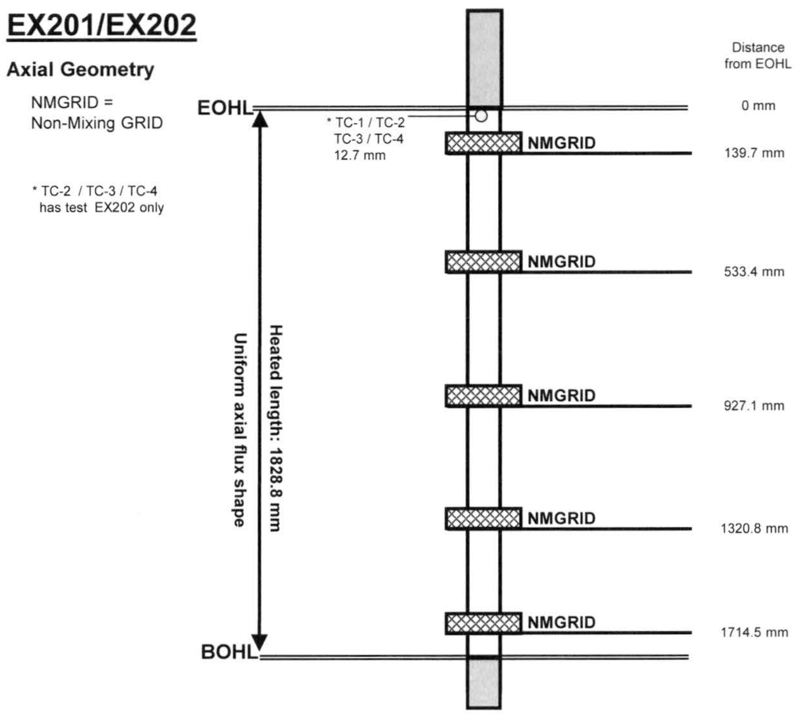

Figure A-26 Axial geometry of CHF test K8800

[ ]

Figure A-27 Axial geometry of CHF test O2400

[

]

Figure A-28 Axial geometry of CHF test SI030

[ ]

Figure A-29 Axial geometry of CHF test SI070

Figure A-30 Axial geometry of CHF test SI140

[ ]

Figure A-31 Axial geometry of CHF test SI160

Figure A-32 Axial geometry of CHF test K2200/K2001/K2002

Figure A-33 Axial geometry of CHF test K2300/K2301

Figure A-34 Axial geometry of CHF test K2402

[

]

Figure A-35 Axial geometry of CHF test K2500

Figure A-36 Axial geometry of CHF test K2600

Figure A-37 Axial geometry of CHF test K2900

[ ]

Figure A-38 Axial geometry of CHF test K3100

Figure A-39 Axial geometry of CHF test K3200

Figure A-40 Axial geometry of CHF test K3800

[ ]

Figure A-41 Axial geometry of CHF test K4000/K4001

[ ]

Figure A-42 Axial geometry of CHF test K9000

[

]

Figure A-43 Axial geometry of CHF test K9100

Figure A-44 Axial geometry of CHF test K9200

Figure A-45 Axial geometry of CHF test K9300

[

]

Figure A-46 Axial geometry of CHF test SI700/SI701

Figure A-47 Axial geometry of CHF test SP010

Figure A-48 Axial geometry of CHF test SP390

Figure A-49 Axial geometry of CHF test SP400

Figure A-50 Axial geometry of CHF test SP480

Figure A-51 Axial geometry of CHF test SP490

Figure A-52 Axial geometry of CHF test SP510

[

]

Figure A-53 Axial geometry of CHF test SP520

[

]

Figure A-54 Axial geometry of CHF test SP530

Figure A-55 Axial geometry of CHF test SP560

Figure A-56 Axial geometry of CHF test SP570

Figure A-57 Axial geometry of CHF test SP590/SP591/SP592

[ ]

Figure A-58 Axial geometry of CHF test SP620

Figure A-59 Axial geometry of CHF test SP630

[ ]

Figure A-60 Axial geometry of CHF test SP650/SP651

[ ]

Figure A-61 Axial geometry of CHF test SP660

[ ]

Figure A-62 Axial geometry of CHF test SP670

Figure A-63 Axial geometry of CHF test SP680

Figure A-64 Axial geometry of CHF test SP690

Appendix B: CHF Test Data

Table B-1 Test assembly conditions for non-mixing grid tests

[ ]

Table B-1 Test assembly conditions for non-mixing grid tests (continued)

[ ]

Table B-1 Test assembly conditions for non-mixing grid tests (continued)

[

]

Table B-1 Test assembly conditions for non-mixing grid tests (continued)

Table B-1 Test assembly conditions for non-mixing grid tests (continued)

[ ]

Table B-1 Test assembly conditions for non-mixing grid tests (continued)

Table B-1 Test assembly conditions for non-mixing grid tests (continued)

[ ]

Table B-1 Test assembly conditions for non-mixing grid tests (continued)

Table B-1 Test assembly conditions for non-mixing grid tests (continued)

[ ]

Table B-1 Test assembly conditions for non-mixing grid tests (continued)

Table B-1 Test assembly conditions for non-mixing grid tests (continued)

Table B-1 Test assembly conditions for non-mixing grid tests (continued)

Table B-1 Test assembly conditions for non-mixing grid tests (continued)

Table B-1 Test assembly conditions for non-mixing grid tests (continued)

Table B-1 Test assembly conditions for non-mixing grid tests (continued)

Table B-1 Test assembly conditions for non-mixing grid tests (continued)

[ ]

Table B-1 Test assembly conditions for non-mixing grid tests (continued)

Table B-1 Test assembly conditions for non-mixing grid tests (continued)

Table B-1 Test assembly conditions for non-mixing grid tests (continued)

Table B-1 Test assembly conditions for non-mixing grid tests (continued)

Table B-1 Test assembly conditions for non-mixing grid tests (continued)

Table B-1 Test assembly conditions for non-mixing grid tests (continued)

[ ]

Table B-1 Test assembly conditions for non-mixing grid tests (continued)

Table B-1 Test assembly conditions for non-mixing grid tests (continued)

Table B-1 Test assembly conditions for non-mixing grid tests (continued)

[ ]

Table B-1 Test assembly conditions for non-mixing grid tests (continued)

Table B-1 Test assembly conditions for non-mixing grid tests (continued)

[ ]

Table B-1 Test assembly conditions for non-mixing grid tests (continued)

[ ]

Table B-1 Test assembly conditions for non-mixing grid tests (continued)

[ ]

Table B-1 Test assembly conditions for non-mixing grid tests (continued)

Table B-1 Test assembly conditions for non-mixing grid tests (continued)

[ ]

Table B-1 Test assembly conditions for non-mixing grid tests (continued)

Table B-1 Test assembly conditions for non-mixing grid tests (continued)

[ ]

Table B-1 Test assembly conditions for non-mixing grid tests (continued)

Table B-1 Test assembly conditions for non-mixing grid tests (continued)

[ ]

Table B-1 Test assembly conditions for non-mixing grid tests (continued)

Table B-1 Test assembly conditions for non-mixing grid tests (continued)

[ ]

Table B-1 Test assembly conditions for non-mixing grid tests (continued)

[ ]

Table B-1 Test assembly conditions for non-mixing grid tests (continued)

Table B-1 Test assembly conditions for non-mixing grid tests (continued)

[ ]

Table B-1 Test assembly conditions for non-mixing grid tests (continued)

Table B-1 Test assembly conditions for non-mixing grid tests (continued)

Table B-1 Test assembly conditions for non-mixing grid tests (continued)

Table B-1 Test assembly conditions for non-mixing grid tests (continued)

Table B-1 Test assembly conditions for non-mixing grid tests (continued)

[ ]

Table B-1 Test assembly conditions for non-mixing grid tests (continued)

Table B-1 Test assembly conditions for non-mixing grid tests (continued)

Table B-1 Test assembly conditions for non-mixing grid tests (continued)

Table B-1 Test assembly conditions for non-mixing grid tests (continued)

Table B-1 Test assembly conditions for non-mixing grid tests (continued)

Table B-1 Test assembly conditions for non-mixing grid tests (continued)

[ ]

Table B-1 Test assembly conditions for non-mixing grid tests (continued)

Table B-1 Test assembly conditions for non-mixing grid tests (continued)

Table B-1 Test assembly conditions for non-mixing grid tests (continued)

[ ]

Table B-1 Test assembly conditions for non-mixing grid tests (continued)

Table B-1 Test assembly conditions for non-mixing grid tests (continued)

Table B-1 Test assembly conditions for non-mixing grid tests (continued)

[ ]

Table B-1 Test assembly conditions for non-mixing grid tests (continued)

Table B-1 Test assembly conditions for non-mixing grid tests (continued)

[

]

Table B-1 Test assembly conditions for non-mixing grid tests (continued)

Table B-1 Test assembly conditions for non-mixing grid tests (continued)

Table B-1 Test assembly conditions for non-mixing grid tests (continued)

Table B-1 Test assembly conditions for non-mixing grid tests (continued)

Table B-1 Test assembly conditions for non-mixing grid tests (continued)

[ ]

Table B-1 Test assembly conditions for non-mixing grid tests (continued)

[ ]

Table B-1 Test assembly conditions for non-mixing grid tests (continued)

Table B-1 Test assembly conditions for non-mixing grid tests (continued)

Table B-1 Test assembly conditions for non-mixing grid tests (continued)

[ ]

Table B-1 Test assembly conditions for non-mixing grid tests (continued)

Table B-1 Test assembly conditions for non-mixing grid tests (continued)

[ ]

Table B-1 Test assembly conditions for non-mixing grid tests (continued)

[ ]

Table B-1 Test assembly conditions for non-mixing grid tests (continued)

Table B-1 Test assembly conditions for non-mixing grid tests (continued)

Table B-1 Test assembly conditions for non-mixing grid tests (continued)

Table B-1 Test assembly conditions for non-mixing grid tests (continued)

Table B-1 Test assembly conditions for non-mixing grid tests (continued)

[

]

Table B-1 Test assembly conditions for non-mixing grid tests (continued)

Table B-1 Test assembly conditions for non-mixing grid tests (continued)

[ ]

Table B-1 Test assembly conditions for non-mixing grid tests (continued)

Table B-1 Test assembly conditions for non-mixing grid tests (continued)

[ ]

Table B-1 Test assembly conditions for non-mixing grid tests (continued)

Table B-1 Test assembly conditions for non-mixing grid tests (continued)

Table B-1 Test assembly conditions for non-mixing grid tests (continued)

[

]

Table B-1 Test assembly conditions for non-mixing grid tests (continued)

[ ]

Table B-1 Test assembly conditions for non-mixing grid tests (continued)

Table B-1 Test assembly conditions for non-mixing grid tests (continued)

Table B-1 Test assembly conditions for non-mixing grid tests (continued)

Table B-1 Test assembly conditions for non-mixing grid tests (continued)

Table B-1 Test assembly conditions for non-mixing grid tests (continued)

Table B-1 Test assembly conditions for non-mixing grid tests (continued)

Table B-1 Test assembly conditions for non-mixing grid tests (continued)

Table B-1 Test assembly conditions for non-mixing grid tests (continued)

Table B-1 Test assembly conditions for non-mixing grid tests (continued)

Table B-1 Test assembly conditions for non-mixing grid tests (continued)

[ ]

Table B-1 Test assembly conditions for non-mixing grid tests (continued)

Table B-1 Test assembly conditions for non-mixing grid tests (continued)

[ ]

Table B-1 Test assembly conditions for non-mixing grid tests (continued)

Table B-1 Test assembly conditions for non-mixing grid tests (continued)

Table B-1 Test assembly conditions for non-mixing grid tests (continued)

Table B-1 Test assembly conditions for non-mixing grid tests (continued)

[ ]

Table B-1 Test assembly conditions for non-mixing grid tests (continued)

Table B-1 Test assembly conditions for non-mixing grid tests (continued)

Table B-1 Test assembly conditions for non-mixing grid tests (continued)

[

]

Table B-1 Test assembly conditions for non-mixing grid tests (continued)

[ ]

Table B-1 Test assembly conditions for non-mixing grid tests (continued)

Table B-1 Test assembly conditions for non-mixing grid tests (continued)

[ ]

Table B-1 Test assembly conditions for non-mixing grid tests (continued)

Table B-1 Test assembly conditions for non-mixing grid tests (continued)

Table B-1 Test assembly conditions for non-mixing grid tests (continued)

[ ]

Table B-1 Test assembly conditions for non-mixing grid tests (continued)

Table B-1 Test assembly conditions for non-mixing grid tests (continued)

[ ]

Table B-1 Test assembly conditions for non-mixing grid tests (continued)

[ ]

Table B-1 Test assembly conditions for non-mixing grid tests (continued)

[ ]

Table B-1 Test assembly conditions for non-mixing grid tests (continued)

Table B-1 Test assembly conditions for non-mixing grid tests (continued)

Table B-1 Test assembly conditions for non-mixing grid tests (continued)

[ ]

Table B-1 Test assembly conditions for non-mixing grid tests (continued)

Table B-1 Test assembly conditions for non-mixing grid tests (continued)

Table B-1 Test assembly conditions for non-mixing grid tests (continued)

[ ]

Table B-1 Test assembly conditions for non-mixing grid tests (continued)

Table B-1 Test assembly conditions for non-mixing grid tests (continued)

Table B-1 Test assembly conditions for non-mixing grid tests (continued)

[ ]

Table B-1 Test assembly conditions for non-mixing grid tests (continued)

[ ]

Table B-1 Test assembly conditions for non-mixing grid tests (continued)

Table B-1 Test assembly conditions for non-mixing grid tests (continued)

[ ]

Table B-1 Test assembly conditions for non-mixing grid tests (continued)

Table B-1 Test assembly conditions for non-mixing grid tests (continued)

Table B-1 Test assembly conditions for non-mixing grid tests (continued)

Table B-1 Test assembly conditions for non-mixing grid tests (continued)

Table B-1 Test assembly conditions for non-mixing grid tests (continued)

[ ]

Table B-1 Test assembly conditions for non-mixing grid tests (continued)

Table B-1 Test assembly conditions for non-mixing grid tests (continued)

Table B-1 Test assembly conditions for non-mixing grid tests (continued)

Table B-1 Test assembly conditions for non-mixing grid tests (continued)

Table B-1 Test assembly conditions for non-mixing grid tests (continued)

[ ]

Table B-1 Test assembly conditions for non-mixing grid tests (continued)

Table B-1 Test assembly conditions for non-mixing grid tests (continued)

Table B-1 Test assembly conditions for non-mixing grid tests (continued)

Table B-1 Test assembly conditions for non-mixing grid tests (continued)

[ ]

Table B-1 Test assembly conditions for non-mixing grid tests (continued)

Table B-1 Test assembly conditions for non-mixing grid tests (continued)

[

]

Table B-1 Test assembly conditions for non-mixing grid tests (continued)

Table B-1 Test assembly conditions for non-mixing grid tests (continued)

Table B-1 Test assembly conditions for non-mixing grid tests (continued)

[ ]

Table B-1 Test assembly conditions for non-mixing grid tests (continued)

Table B-1 Test assembly conditions for non-mixing grid tests (continued)

Table B-1 Test assembly conditions for non-mixing grid tests (continued)

[ ]

Table B-1 Test assembly conditions for non-mixing grid tests (continued)

Table B-1 Test assembly conditions for non-mixing grid tests (continued)

Table B-1 Test assembly conditions for non-mixing grid tests (continued)

[ ]

Table B-1 Test assembly conditions for non-mixing grid tests (continued)

Table B-1 Test assembly conditions for non-mixing grid tests (continued)

Table B-1 Test assembly conditions for non-mixing grid tests (continued)

Table B-1 Test assembly conditions for non-mixing grid tests (continued)

Table B-2 Test assembly conditions for HTP grid tests

[ ]

Table B-2 Test assembly conditions for HTP grid tests (continued)

[

]

Table B-2 Test assembly conditions for HTP grid tests (continued)

Table B-2 Test assembly conditions for HTP grid tests (continued)

[ ]

Table B-2 Test assembly conditions for HTP grid tests (continued)

Table B-2 Test assembly conditions for HTP grid tests (continued)

[ ]

Table B-2 Test assembly conditions for HTP grid tests (continued)

Table B-2 Test assembly conditions for HTP grid tests (continued)

[ ]

Table B-2 Test assembly conditions for HTP grid tests (continued)

Table B-2 Test assembly conditions for HTP grid tests (continued)

Table B-2 Test assembly conditions for HTP grid tests (continued)

Table B-2 Test assembly conditions for HTP grid tests (continued)

Table B-2 Test assembly conditions for HTP grid tests (continued)

[ ]

Table B-2 Test assembly conditions for HTP grid tests (continued)

Table B-2 Test assembly conditions for HTP grid tests (continued)

[

]

Table B-2 Test assembly conditions for HTP grid tests (continued)

Table B-2 Test assembly conditions for HTP grid tests (continued)

[ ]

Table B-2 Test assembly conditions for HTP grid tests (continued)

[ ]

Table B-2 Test assembly conditions for HTP grid tests (continued)

Table B-2 Test assembly conditions for HTP grid tests (continued)

Table B-2 Test assembly conditions for HTP grid tests (continued)

[ ]

Table B-2 Test assembly conditions for HTP grid tests (continued)

Table B-2 Test assembly conditions for HTP grid tests (continued)

[ ]

Table B-2 Test assembly conditions for HTP grid tests (continued)

[ ]

Table B-2 Test assembly conditions for HTP grid tests (continued)

[ ]

Table B-2 Test assembly conditions for HTP grid tests (continued)

Table B-2 Test assembly conditions for HTP grid tests (continued)

Table B-2 Test assembly conditions for HTP grid tests (continued)

Table B-2 Test assembly conditions for HTP grid tests (continued)

[ ]

Table B-2 Test assembly conditions for HTP grid tests (continued)

[

]

Table B-2 Test assembly conditions for HTP grid tests (continued)

Table B-2 Test assembly conditions for HTP grid tests (continued)

Table B-2 Test assembly conditions for HTP grid tests (continued)

[ ]

Table B-2 Test assembly conditions for HTP grid tests (continued)

[ ]

Table B-2 Test assembly conditions for HTP grid tests (continued)

Table B-2 Test assembly conditions for HTP grid tests (continued)

Table B-2 Test assembly conditions for HTP grid tests (continued)

Table B-2 Test assembly conditions for HTP grid tests (continued)

[ ]

Table B-2 Test assembly conditions for HTP grid tests (continued)

Table B-2 Test assembly conditions for HTP grid tests (continued)

Table B-2 Test assembly conditions for HTP grid tests (continued)

Table B-2 Test assembly conditions for HTP grid tests (continued)

Table B-2 Test assembly conditions for HTP grid tests (continued)

[

]

Table B-2 Test assembly conditions for HTP grid tests (continued)

[ ]

Table B-2 Test assembly conditions for HTP grid tests (continued)

[ ]

Table B-2 Test assembly conditions for HTP grid tests (continued)

Table B-2 Test assembly conditions for HTP grid tests (continued)

Table B-2 Test assembly conditions for HTP grid tests (continued)

Table B-2 Test assembly conditions for HTP grid tests (continued)

[ ]

Table B-2 Test assembly conditions for HTP grid tests (continued)

Table B-2 Test assembly conditions for HTP grid tests (continued)

[ ]

Table B-2 Test assembly conditions for HTP grid tests (continued)

[ ]

Table B-2 Test assembly conditions for HTP grid tests (continued)

Table B-2 Test assembly conditions for HTP grid tests (continued)

Table B-2 Test assembly conditions for HTP grid tests (continued)

[ ]

Table B-2 Test assembly conditions for HTP grid tests (continued)

Table B-2 Test assembly conditions for HTP grid tests (continued)

[ ]

Table B-2 Test assembly conditions for HTP grid tests (continued)

Table B-2 Test assembly conditions for HTP grid tests (continued)

[ ]

Table B-2 Test assembly conditions for HTP grid tests (continued)

Table B-2 Test assembly conditions for HTP grid tests (continued)

Table B-2 Test assembly conditions for HTP grid tests (continued)

[ ]

Table B-2 Test assembly conditions for HTP grid tests (continued)

Table B-2 Test assembly conditions for HTP grid tests (continued)

Table B-2 Test assembly conditions for HTP grid tests (continued)

Table B-2 Test assembly conditions for HTP grid tests (continued)

[ ]

Table B-2 Test assembly conditions for HTP grid tests (continued)

Table B-2 Test assembly conditions for HTP grid tests (continued)

Table B-2 Test assembly conditions for HTP grid tests (continued)

Table B-2 Test assembly conditions for HTP grid tests (continued)

Table B-2 Test assembly conditions for HTP grid tests (continued)

Table B-2 Test assembly conditions for HTP grid tests (continued)

[ ]

Table B-2 Test assembly conditions for HTP grid tests (continued)

Table B-2 Test assembly conditions for HTP grid tests (continued)

[ ]

Table B-2 Test assembly conditions for HTP grid tests (continued)

Table B-2 Test assembly conditions for HTP grid tests (continued)

Table B-2 Test assembly conditions for HTP grid tests (continued)

Table B-2 Test assembly conditions for HTP grid tests (continued)

Table B-2 Test assembly conditions for HTP grid tests (continued)

[ ]

Table B-2 Test assembly conditions for HTP grid tests (continued)

Table B-2 Test assembly conditions for HTP grid tests (continued)

[ ]

Table B-2 Test assembly conditions for HTP grid tests (continued)

Table B-2 Test assembly conditions for HTP grid tests (continued)

Table B-2 Test assembly conditions for HTP grid tests (continued)

[ ]

Table B-2 Test assembly conditions for HTP grid tests (continued)

Table B-2 Test assembly conditions for HTP grid tests (continued)

Table B-2 Test assembly conditions for HTP grid tests (continued)

Table B-2 Test assembly conditions for HTP grid tests (continued)

Table B-2 Test assembly conditions for HTP grid tests (continued)

Table B-2 Test assembly conditions for HTP grid tests (continued)

Table B-2 Test assembly conditions for HTP grid tests (continued)

[ ]

Table B-2 Test assembly conditions for HTP grid tests (continued)

[ ]

Table B-2 Test assembly conditions for HTP grid tests (continued)

Table B-2 Test assembly conditions for HTP grid tests (continued)

[ ]

Table B-2 Test assembly conditions for HTP grid tests (continued)

Table B-2 Test assembly conditions for HTP grid tests (continued)

Table B-2 Test assembly conditions for HTP grid tests (continued)

Table B-2 Test assembly conditions for HTP grid tests (continued)

Table B-2 Test assembly conditions for HTP grid tests (continued)

[ ]

Table B-2 Test assembly conditions for HTP grid tests (continued)

Table B-2 Test assembly conditions for HTP grid tests (continued)

Table B-2 Test assembly conditions for HTP grid tests (continued)

Table B-2 Test assembly conditions for HTP grid tests (continued)

Table B-2 Test assembly conditions for HTP grid tests (continued)

[ ]

Table B-2 Test assembly conditions for HTP grid tests (continued)

[ ]

Table B-2 Test assembly conditions for HTP grid tests (continued)

Table B-2 Test assembly conditions for HTP grid tests (continued)

Table B-2 Test assembly conditions for HTP grid tests (continued)

Table B-2 Test assembly conditions for HTP grid tests (continued)

Table B-2 Test assembly conditions for HTP grid tests (continued)

Table B-2 Test assembly conditions for HTP grid tests (continued)

[ ]

Table B-2 Test assembly conditions for HTP grid tests (continued)

Table B-2 Test assembly conditions for HTP grid tests (continued)

Table B-2 Test assembly conditions for HTP grid tests (continued)

Table B-2 Test assembly conditions for HTP grid tests (continued)

[ ]

Table B-2 Test assembly conditions for HTP grid tests (continued)

Table B-2 Test assembly conditions for HTP grid tests (continued)

[ ]

Table B-2 Test assembly conditions for HTP grid tests (continued)

Table B-2 Test assembly conditions for HTP grid tests (continued)

[ ]

Table B-2 Test assembly conditions for HTP grid tests (continued)

Table B-2 Test assembly conditions for HTP grid tests (continued)

[ ]

Table B-2 Test assembly conditions for HTP grid tests (continued)

Table B-2 Test assembly conditions for HTP grid tests (continued)

Table B-2 Test assembly conditions for HTP grid tests (continued)

Table B-2 Test assembly conditions for HTP grid tests (continued)

[ ]

Table B-2 Test assembly conditions for HTP grid tests (continued)

Table B-2 Test assembly conditions for HTP grid tests (continued)

Table B-2 Test assembly conditions for HTP grid tests (continued)

Table B-2 Test assembly conditions for HTP grid tests (continued)

[ ]

Table B-2 Test assembly conditions for HTP grid tests (continued)

[ ]

Table B-2 Test assembly conditions for HTP grid tests (continued)

Table B-2 Test assembly conditions for HTP grid tests (continued)

Table B-2 Test assembly conditions for HTP grid tests (continued)

Table B-2 Test assembly conditions for HTP grid tests (continued)

Table B-2 Test assembly conditions for HTP grid tests (continued)

Table B-2 Test assembly conditions for HTP grid tests (continued)

Table B-2 Test assembly conditions for HTP grid tests (continued)

[ ]

Table B-2 Test assembly conditions for HTP grid tests (continued)

[ ]

Table B-2 Test assembly conditions for HTP grid tests (continued)

[ ]

Table B-2 Test assembly conditions for HTP grid tests (continued)

Table B-2 Test assembly conditions for HTP grid tests (continued)

Table B-2 Test assembly conditions for HTP grid tests (continued)

Table B-2 Test assembly conditions for HTP grid tests (continued)

Table B-2 Test assembly conditions for HTP grid tests (continued)

Table B-2 Test assembly conditions for HTP grid tests (continued)

[ ]

Table B-2 Test assembly conditions for HTP grid tests (continued)

[ ]

Table B-2 Test assembly conditions for HTP grid tests (continued)

Table B-3 Local conditions from COBRA-FLX simulations for grid tests

Table B-3 Local conditions from COBRA-FLX simulations for grid tests (continued)

[ ]

Table B-3 Local conditions from COBRA-FLX simulations for grid tests (continued)

[ ]

Table B-3 Local conditions from COBRA-FLX simulations for grid tests (continued)

Table B-3 Local conditions from COBRA-FLX simulations for grid tests (continued)

Table B-3 Local conditions from COBRA-FLX simulations for grid tests (continued)

Table B-3 Local conditions from COBRA-FLX simulations for grid tests (continued)

Table B-3 Local conditions from COBRA-FLX simulations for grid tests (continued)

Table B-3 Local conditions from COBRA-FLX simulations for grid tests (continued)

[ ]

Table B-3 Local conditions from COBRA-FLX simulations for grid tests (continued)

Table B-3 Local conditions from COBRA-FLX simulations for grid tests (continued)

Table B-3 Local conditions from COBRA-FLX simulations for grid tests (continued)

Table B-3 Local conditions from COBRA-FLX simulations for grid tests (continued)

[ ]

Table B-3 Local conditions from COBRA-FLX simulations for grid tests (continued)

[ ]

Table B-3 Local conditions from COBRA-FLX simulations for grid tests (continued)

Table B-3 Local conditions from COBRA-FLX simulations for grid tests (continued)

[ ]

Table B-3 Local conditions from COBRA-FLX simulations for grid tests (continued)

Table B-3 Local conditions from COBRA-FLX simulations for grid tests (continued)

Table B-3 Local conditions from COBRA-FLX simulations for grid tests (continued)

Table B-3 Local conditions from COBRA-FLX simulations for grid tests (continued)

Table B-3 Local conditions from COBRA-FLX simulations for grid tests (continued)

Table B-3 Local conditions from COBRA-FLX simulations for grid tests (continued)

Table B-3 Local conditions from COBRA-FLX simulations for grid tests (continued)

Table B-3 Local conditions from COBRA-FLX simulations for grid tests (continued)

Table B-3 Local conditions from COBRA-FLX simulations for grid tests (continued)

Table B-3 Local conditions from COBRA-FLX simulations for grid tests (continued)

Table B-3 Local conditions from COBRA-FLX simulations for grid tests (continued)

Table B-3 Local conditions from COBRA-FLX simulations for grid tests (continued)

Table B-3 Local conditions from COBRA-FLX simulations for grid tests (continued)

[ ]

Table B-3 Local conditions from COBRA-FLX simulations for grid tests (continued)

Table B-3 Local conditions from COBRA-FLX simulations for grid tests (continued)

Table B-3 Local conditions from COBRA-FLX simulations for grid tests (continued)

Table B-3 Local conditions from COBRA-FLX simulations for grid tests (continued)

[ ]

Table B-3 Local conditions from COBRA-FLX simulations for grid tests (continued)

[ ]

Table B-3 Local conditions from COBRA-FLX simulations for grid tests (continued)

[ ]

Table B-3 Local conditions from COBRA-FLX simulations for grid tests (continued)

Table B-3 Local conditions from COBRA-FLX simulations for grid tests (continued)

Table B-3 Local conditions from COBRA-FLX simulations for grid tests (continued)

Table B-3 Local conditions from COBRA-FLX simulations for grid tests (continued)

[ ]

Table B-3 Local conditions from COBRA-FLX simulations for grid tests (continued)

[ ]

Table B-3 Local conditions from COBRA-FLX simulations for grid tests (continued)

Table B-3 Local conditions from COBRA-FLX simulations for grid tests (continued)

Table B-3 Local conditions from COBRA-FLX simulations for grid tests (continued)

Table B-3 Local conditions from COBRA-FLX simulations for grid tests (continued)

[ ]

Table B-3 Local conditions from COBRA-FLX simulations for grid tests (continued)

Table B-3 Local conditions from COBRA-FLX simulations for grid tests (continued)

Table B-3 Local conditions from COBRA-FLX simulations for grid tests (continued)

Table B-3 Local conditions from COBRA-FLX simulations for grid tests (continued)

Table B-3 Local conditions from COBRA-FLX simulations for grid tests (continued)

Table B-3 Local conditions from COBRA-FLX simulations for grid tests (continued)

Table B-3 Local conditions from COBRA-FLX simulations for grid tests (continued)

Table B-3 Local conditions from COBRA-FLX simulations for grid tests (continued)

Table B-3 Local conditions from COBRA-FLX simulations for grid tests (continued)

[ ]

Table B-3 Local conditions from COBRA-FLX simulations for grid tests (continued)

Table B-3 Local conditions from COBRA-FLX simulations for grid tests (continued)

Table B-3 Local conditions from COBRA-FLX simulations for grid tests (continued)

[ ]

Table B-3 Local conditions from COBRA-FLX simulations for grid tests (continued)

Table B-3 Local conditions from COBRA-FLX simulations for grid tests (continued)

Table B-3 Local conditions from COBRA-FLX simulations for grid tests (continued)

Table B-3 Local conditions from COBRA-FLX simulations for grid tests (continued)

[ ]

Table B-3 Local conditions from COBRA-FLX simulations for grid tests (continued)

Table B-3 Local conditions from COBRA-FLX simulations for grid tests (continued)

Table B-3 Local conditions from COBRA-FLX simulations for grid tests (continued)

Table B-3 Local conditions from COBRA-FLX simulations for grid tests (continued)

Table B-3 Local conditions from COBRA-FLX simulations for grid tests (continued)

Table B-3 Local conditions from COBRA-FLX simulations for grid tests (continued)

Table B-3 Local conditions from COBRA-FLX simulations for grid tests (continued)

Table B-3 Local conditions from COBRA-FLX simulations for grid tests (continued)

Table B-3 Local conditions from COBRA-FLX simulations for grid tests (continued)

Table B-3 Local conditions from COBRA-FLX simulations for grid tests (continued)

Table B-3 Local conditions from COBRA-FLX simulations for grid tests (continued)

Table B-3 Local conditions from COBRA-FLX simulations for grid tests (continued)

Table B-3 Local conditions from COBRA-FLX simulations for grid tests (continued)

Table B-3 Local conditions from COBRA-FLX simulations for grid tests (continued)

Table B-3 Local conditions from COBRA-FLX simulations for grid tests (continued)

Table B-3 Local conditions from COBRA-FLX simulations for grid tests (continued)

Table B-3 Local conditions from COBRA-FLX simulations for grid tests (continued)

Table B-3 Local conditions from COBRA-FLX simulations for grid tests (continued)

[ ]

Table B-3 Local conditions from COBRA-FLX simulations for grid tests (continued)

[ ]

Table B-3 Local conditions from COBRA-FLX simulations for grid tests (continued)

Table B-3 Local conditions from COBRA-FLX simulations for grid tests (continued)

Table B-3 Local conditions from COBRA-FLX simulations for grid tests (continued)

Table B-3 Local conditions from COBRA-FLX simulations for grid tests (continued)

Table B-3 Local conditions from COBRA-FLX simulations for grid tests (continued)

Table B-3 Local conditions from COBRA-FLX simulations for grid tests (continued)

[ ]

Table B-3 Local conditions from COBRA-FLX simulations for grid tests (continued)

Table B-3 Local conditions from COBRA-FLX simulations for grid tests (continued)

Table B-3 Local conditions from COBRA-FLX simulations for grid tests (continued)

Table B-3 Local conditions from COBRA-FLX simulations for grid tests (continued)

Table B-3 Local conditions from COBRA-FLX simulations for grid tests (continued)

Table B-3 Local conditions from COBRA-FLX simulations for grid tests (continued)

Table B-3 Local conditions from COBRA-FLX simulations for grid tests (continued)

Table B-3 Local conditions from COBRA-FLX simulations for grid tests (continued)

Table B-3 Local conditions from COBRA-FLX simulations for grid tests (continued)

Table B-3 Local conditions from COBRA-FLX simulations for grid tests (continued)

Table B-3 Local conditions from COBRA-FLX simulations for grid tests (continued)

Table B-3 Local conditions from COBRA-FLX simulations for grid tests (continued)

Table B-3 Local conditions from COBRA-FLX simulations for grid tests (continued)

Table B-3 Local conditions from COBRA-FLX simulations for grid tests (continued)

[

]

Table B-3 Local conditions from COBRA-FLX simulations for grid tests (continued)

[ ]

Table B-3 Local conditions from COBRA-FLX simulations for grid tests (continued)

Table B-3 Local conditions from COBRA-FLX simulations for grid tests (continued)

Table B-3 Local conditions from COBRA-FLX simulations for grid tests (continued)

Table B-3 Local conditions from COBRA-FLX simulations for grid tests (continued)

Table B-3 Local conditions from COBRA-FLX simulations for grid tests (continued)

Table B-3 Local conditions from COBRA-FLX simulations for grid tests (continued)

Table B-3 Local conditions from COBRA-FLX simulations for grid tests (continued)

Table B-3 Local conditions from COBRA-FLX simulations for grid tests (continued)

Table B-3 Local conditions from COBRA-FLX simulations for grid tests (continued)

Table B-3 Local conditions from COBRA-FLX simulations for grid tests (continued)

[ ]

Table B-3 Local conditions from COBRA-FLX simulations for grid tests (continued)

[ ]

Table B-3 Local conditions from COBRA-FLX simulations for grid tests (continued)

Table B-3 Local conditions from COBRA-FLX simulations for grid tests (continued)

Table B-3 Local conditions from COBRA-FLX simulations for grid tests (continued)

Table B-3 Local conditions from COBRA-FLX simulations for grid tests (continued)

Table B-3 Local conditions from COBRA-FLX simulations for grid tests (continued)

Table B-3 Local conditions from COBRA-FLX simulations for grid tests (continued)

[ ]

Table B-3 Local conditions from COBRA-FLX simulations for grid tests (continued)

Table B-3 Local conditions from COBRA-FLX simulations for grid tests (continued)

Table B-3 Local conditions from COBRA-FLX simulations for grid tests (continued)

Table B-3 Local conditions from COBRA-FLX simulations for grid tests (continued)

Table B-3 Local conditions from COBRA-FLX simulations for grid tests (continued)

[ ]

Table B-3 Local conditions from COBRA-FLX simulations for grid tests (continued)

Table B-3 Local conditions from COBRA-FLX simulations for grid tests (continued)

Table B-3 Local conditions from COBRA-FLX simulations for grid tests (continued)

Table B-3 Local conditions from COBRA-FLX simulations for grid tests (continued)

Table B-3 Local conditions from COBRA-FLX simulations for grid tests (continued)

Table B-3 Local conditions from COBRA-FLX simulations for grid tests (continued)

[ ]

Table B-3 Local conditions from COBRA-FLX simulations for grid tests (continued)

Table B-3 Local conditions from COBRA-FLX simulations for grid tests (continued)

Table B-3 Local conditions from COBRA-FLX simulations for grid tests (continued)

Table B-3 Local conditions from COBRA-FLX simulations for grid tests (continued)

Table B-3 Local conditions from COBRA-FLX simulations for grid tests (continued)

Table B-3 Local conditions from COBRA-FLX simulations for grid tests (continued)

Table B-3 Local conditions from COBRA-FLX simulations for grid tests (continued)

Table B-3 Local conditions from COBRA-FLX simulations for grid tests (continued)

Table B-3 Local conditions from COBRA-FLX simulations for grid tests (continued)

Table B-3 Local conditions from COBRA-FLX simulations for grid tests (continued)

Table B-3 Local conditions from COBRA-FLX simulations for grid tests (continued)

Table B-3 Local conditions from COBRA-FLX simulations for grid tests (continued)

Table B-3 Local conditions from COBRA-FLX simulations for grid tests (continued)

Table B-3 Local conditions from COBRA-FLX simulations for grid tests (continued)

Table B-3 Local conditions from COBRA-FLX simulations for grid tests (continued)

Table B-3 Local conditions from COBRA-FLX simulations for grid tests (continued)

Table B-3 Local conditions from COBRA-FLX simulations for grid tests (continued)

Table B-3 Local conditions from COBRA-FLX simulations for grid tests (continued)

[ ]

Table B-3 Local conditions from COBRA-FLX simulations for grid tests (continued)

Table B-3 Local conditions from COBRA-FLX simulations for grid tests (continued)

Table B-3 Local conditions from COBRA-FLX simulations for grid tests (continued)

[ ]

Table B-3 Local conditions from COBRA-FLX simulations for grid tests (continued)

Table B-3 Local conditions from COBRA-FLX simulations for grid tests (continued)

Table B-3 Local conditions from COBRA-FLX simulations for grid tests (continued)

[ ]

Table B-3 Local conditions from COBRA-FLX simulations for grid tests (continued)

Table B-3 Local conditions from COBRA-FLX simulations for grid tests (continued)

Table B-3 Local conditions from COBRA-FLX simulations for grid tests (continued)

Table B-3 Local conditions from COBRA-FLX simulations for grid tests (continued)

Table B-3 Local conditions from COBRA-FLX simulations for grid tests (continued)

Table B-3 Local conditions from COBRA-FLX simulations for grid tests (continued)

Table B-3 Local conditions from COBRA-FLX simulations for grid tests (continued)

Table B-3 Local conditions from COBRA-FLX simulations for grid tests (continued)

Table B-3 Local conditions from COBRA-FLX simulations for grid tests (continued)

Table B-3 Local conditions from COBRA-FLX simulations for grid tests (continued)

Table B-3 Local conditions from COBRA-FLX simulations for grid tests (continued)

Table B-3 Local conditions from COBRA-FLX simulations for grid tests (continued)

Table B-3 Local conditions from COBRA-FLX simulations for grid tests (continued)

[ ]

Table B-3 Local conditions from COBRA-FLX simulations for grid tests (continued)

Table B-3 Local conditions from COBRA-FLX simulations for grid tests (continued)

Table B-3 Local conditions from COBRA-FLX simulations for grid tests (continued)

Table B-3 Local conditions from COBRA-FLX simulations for grid tests (continued)

Table B-3 Local conditions from COBRA-FLX simulations for grid tests (continued)

Table B-3 Local conditions from COBRA-FLX simulations for grid tests (continued)

[ ]

Table B-3 Local conditions from COBRA-FLX simulations for grid tests (continued)

Table B-3 Local conditions from COBRA-FLX simulations for grid tests (continued)

Table B-3 Local conditions from COBRA-FLX simulations for grid tests (continued)

Table B-3 Local conditions from COBRA-FLX simulations for grid tests (continued)

[

]

Table B-3 Local conditions from COBRA-FLX simulations for grid tests (continued)

Table B-3 Local conditions from COBRA-FLX simulations for grid tests (continued)

Table B-3 Local conditions from COBRA-FLX simulations for grid tests (continued)

[ ]

Table B-3 Local conditions from COBRA-FLX simulations for grid tests (continued)

Table B-3 Local conditions from COBRA-FLX simulations for grid tests (continued)

Table B-3 Local conditions from COBRA-FLX simulations for grid tests (continued)

[ ]

Table B-3 Local conditions from COBRA-FLX simulations for grid tests (continued)

Table B-3 Local conditions from COBRA-FLX simulations for grid tests (continued)

Table B-3 Local conditions from COBRA-FLX simulations for grid tests (continued)

[ ]

Table B-3 Local conditions from COBRA-FLX simulations for grid tests (continued)

Table B-3 Local conditions from COBRA-FLX simulations for grid tests (continued)

Table B-3 Local conditions from COBRA-FLX simulations for grid tests (continued)

Table B-3 Local conditions from COBRA-FLX simulations for grid tests (continued)

Table B-3 Local conditions from COBRA-FLX simulations for grid tests (continued)

Table B-3 Local conditions from COBRA-FLX simulations for grid tests (continued)

[ ]

Table B-3 Local conditions from COBRA-FLX simulations for grid tests (continued)

Table B-3 Local conditions from COBRA-FLX simulations for grid tests (continued)

[ ]

Table B-3 Local conditions from COBRA-FLX simulations for grid tests (continued)

Table B-3 Local conditions from COBRA-FLX simulations for grid tests (continued)

Table B-3 Local conditions from COBRA-FLX simulations for grid tests (continued)

Table B-3 Local conditions from COBRA-FLX simulations for grid tests (continued)

[ ]

Table B-3 Local conditions from COBRA-FLX simulations for grid tests (continued)

Table B-3 Local conditions from COBRA-FLX simulations for grid tests (continued)

Table B-3 Local conditions from COBRA-FLX simulations for grid tests (continued)

Table B-3 Local conditions from COBRA-FLX simulations for grid tests (continued)

Table B-3 Local conditions from COBRA-FLX simulations for grid tests (continued)

Table B-3 Local conditions from COBRA-FLX simulations for grid tests (continued)

Table B-3 Local conditions from COBRA-FLX simulations for grid tests (continued)

Table B-3 Local conditions from COBRA-FLX simulations for grid tests (continued)

Table B-3 Local conditions from COBRA-FLX simulations for grid tests (continued)

Table B-3 Local conditions from COBRA-FLX simulations for grid tests (continued)

Table B-3 Local conditions from COBRA-FLX simulations for grid tests (continued)

Table B-3 Local conditions from COBRA-FLX simulations for grid tests (continued)

Table B-3 Local conditions from COBRA-FLX simulations for grid tests (continued)

[ ]

Table B-3 Local conditions from COBRA-FLX simulations for grid tests (continued)

Table B-3 Local conditions from COBRA-FLX simulations for grid tests (continued)

[ ]

Table B-3 Local conditions from COBRA-FLX simulations for grid tests (continued)

Table B-3 Local conditions from COBRA-FLX simulations for grid tests (continued)

Table B-3 Local conditions from COBRA-FLX simulations for grid tests (continued)

Table B-3 Local conditions from COBRA-FLX simulations for grid tests (continued)

Table B-3 Local conditions from COBRA-FLX simulations for grid tests (continued)

Table B-3 Local conditions from COBRA-FLX simulations for grid tests (continued)

Table B-3 Local conditions from COBRA-FLX simulations for grid tests (continued)

Table B-3 Local conditions from COBRA-FLX simulations for grid tests (continued)

Table B-3 Local conditions from COBRA-FLX simulations for grid tests (continued)

Table B-3 Local conditions from COBRA-FLX simulations for grid tests (continued)

[ ]

Table B-3 Local conditions from COBRA-FLX simulations for grid tests (continued)

Table B-3 Local conditions from COBRA-FLX simulations for grid tests (continued)

Table B-3 Local conditions from COBRA-FLX simulations for grid tests (continued)

Table B-3 Local conditions from COBRA-FLX simulations for grid tests (continued)

[ ]

Table B-3 Local conditions from COBRA-FLX simulations for grid tests (continued)

Table B-3 Local conditions from COBRA-FLX simulations for grid tests (continued)

Table B-3 Local conditions from COBRA-FLX simulations for grid tests (continued)

Table B-3 Local conditions from COBRA-FLX simulations for grid tests (continued)

[

]

Table B-3 Local conditions from COBRA-FLX simulations for grid tests (continued)

[ ]

Table B-3 Local conditions from COBRA-FLX simulations for grid tests (continued)

Table B-3 Local conditions from COBRA-FLX simulations for grid tests (continued)

Table B-3 Local conditions from COBRA-FLX simulations for grid tests (continued)

Table B-3 Local conditions from COBRA-FLX simulations for grid tests (continued)

Table B-3 Local conditions from COBRA-FLX simulations for grid tests (continued)

Table B-3 Local conditions from COBRA-FLX simulations for grid tests (continued)

[ ]

Table B-3 Local conditions from COBRA-FLX simulations for grid tests (continued)

Table B-3 Local conditions from COBRA-FLX simulations for grid tests (continued)

Table B-3 Local conditions from COBRA-FLX simulations for grid tests (continued)

[ ]

Table B-3 Local conditions from COBRA-FLX simulations for grid tests (continued)

Table B-3 Local conditions from COBRA-FLX simulations for grid tests (continued)

Table B-3 Local conditions from COBRA-FLX simulations for grid tests (continued)

Table B-3 Local conditions from COBRA-FLX simulations for grid tests (continued)

Table B-3 Local conditions from COBRA-FLX simulations for grid tests (continued)

Table B-3 Local conditions from COBRA-FLX simulations for grid tests (continued)

Table B-3 Local conditions from COBRA-FLX simulations for grid tests (continued)

Table B-3 Local conditions from COBRA-FLX simulations for grid tests (continued)

Table B-3 Local conditions from COBRA-FLX simulations for grid tests (continued)

Table B-3 Local conditions from COBRA-FLX simulations for grid tests (continued)

Table B-3 Local conditions from COBRA-FLX simulations for grid tests (continued)

Table B-3 Local conditions from COBRA-FLX simulations for grid tests (continued)

Table B-3 Local conditions from COBRA-FLX simulations for grid tests (continued)

Table B-3 Local conditions from COBRA-FLX simulations for grid tests (continued)

Table B-3 Local conditions from COBRA-FLX simulations for grid tests (continued)

Table B-3 Local conditions from COBRA-FLX simulations for grid tests (continued)

Table B-3 Local conditions from COBRA-FLX simulations for grid tests (continued)

Table B-3 Local conditions from COBRA-FLX simulations for grid tests (continued)

Table B-3 Local conditions from COBRA-FLX simulations for grid tests (continued)

Table B-3 Local conditions from COBRA-FLX simulations for grid tests (continued)

Table B-3 Local conditions from COBRA-FLX simulations for grid tests (continued)

Table B-3 Local conditions from COBRA-FLX simulations for grid tests (continued)

Table B-3 Local conditions from COBRA-FLX simulations for grid tests (continued)

Table B-3 Local conditions from COBRA-FLX simulations for grid tests (continued)

Table B-3 Local conditions from COBRA-FLX simulations for grid tests (continued)

Table B-3 Local conditions from COBRA-FLX simulations for grid tests (continued)

Table B-3 Local conditions from COBRA-FLX simulations for grid tests (continued)

Table B-3 Local conditions from COBRA-FLX simulations for grid tests (continued)

Table B-3 Local conditions from COBRA-FLX simulations for grid tests (continued)

Table B-3 Local conditions from COBRA-FLX simulations for grid tests (continued)

Table B-3 Local conditions from COBRA-FLX simulations for grid tests (continued)

[

]

Table B-3 Local conditions from COBRA-FLX simulations for grid tests (continued)

Table B-3 Local conditions from COBRA-FLX simulations for grid tests (continued)

Table B-3 Local conditions from COBRA-FLX simulations for grid tests (continued)

Table B-3 Local conditions from COBRA-FLX simulations for grid tests (continued)

[ ]

Table B-3 Local conditions from COBRA-FLX simulations for grid tests (continued)

Table B-3 Local conditions from COBRA-FLX simulations for grid tests (continued)

Table B-3 Local conditions from COBRA-FLX simulations for grid tests (continued)

Table B-3 Local conditions from COBRA-FLX simulations for grid tests (continued)

Table B-3 Local conditions from COBRA-FLX simulations for grid tests (continued)

Table B-3 Local conditions from COBRA-FLX simulations for grid tests (continued)

Table B-3 Local conditions from COBRA-FLX simulations for grid tests (continued)

Table B-3 Local conditions from COBRA-FLX simulations for grid tests (continued)

[

]

Table B-3 Local conditions from COBRA-FLX simulations for grid tests (continued)

Table B-3 Local conditions from COBRA-FLX simulations for grid tests (continued)

Table B-3 Local conditions from COBRA-FLX simulations for grid tests (continued)

[

]

Table B-3 Local conditions from COBRA-FLX simulations for grid tests (continued)

[ ]

Table B-3 Local conditions from COBRA-FLX simulations for grid tests (continued)

Table B-3 Local conditions from COBRA-FLX simulations for grid tests (continued)

Table B-3 Local conditions from COBRA-FLX simulations for grid tests (continued)

Table B-3 Local conditions from COBRA-FLX simulations for grid tests (continued)

[ ]

Table B-3 Local conditions from COBRA-FLX simulations for grid tests (continued)

Table B-3 Local conditions from COBRA-FLX simulations for grid tests (continued)

[

]

Table B-3 Local conditions from COBRA-FLX simulations for grid tests (continued)

Table B-3 Local conditions from COBRA-FLX simulations for grid tests (continued)

Table B-3 Local conditions from COBRA-FLX simulations for grid tests (continued)

Table B-3 Local conditions from COBRA-FLX simulations for grid tests (continued)

[ ]

Table B-3 Local conditions from COBRA-FLX simulations for grid tests (continued)

[ ]

Table B-3 Local conditions from COBRA-FLX simulations for grid tests (continued)

Table B-3 Local conditions from COBRA-FLX simulations for grid tests (continued)

[ ]

Table B-3 Local conditions from COBRA-FLX simulations for grid tests (continued)

Table B-3 Local conditions from COBRA-FLX simulations for grid tests (continued)